Vol. 130, No. 2 The American Naturalist August 1987

SWARMS OF PREDATORS EXHIBIT "PREYTAXIS" IF INDIVIDUAL PREDATORS USE AREA-RESTRICTED SEARCH

PETER KAREIVA AND GARRETT ODELL

Department of Zoology, NJ-15, University of Washington, Seattle, Washington 98195

Submitted June 3, 1985; Revised August 15, 1986; Accepted November 21, 1986

Virtually all predators search more thoroughly for food in some areas than they do in other areas. This uneven searching effort, often a response to spatial variation in prey density (Curio 1976), may lead to predation rates that are greater in regions where prey are more abundant (i.e., density-dependent predation). Much confusion stems from the phenomenological nature of existing models that have been used to represent nonrandom foraging (see Hassell and May 1974 for one pioneering exception to this trend). Because these models (reviewed in Hassell 1978; Hassell and May 1985; Chesson and Murdoch 1986) start with an alleged outcome of nonrandom foraging rather than with a model of the process itself, and because they never explicitly represent animals moving through a spatial environment, their conclusions are difficult to relate to actual behavioral patterns. Field experiments have also tended to neglect the details of how predators forage, concentrating instead on outcomes such as spatial patterns of predator or parasite incidence (Heads and Lawton 1983; Murdoch et al. 1985). There are good logistical reasons for avoiding the details of how an animal moves in pursuit of food; these details make the mathematical analysis more difficult and complicate both the design and interpretation of field observations (Kareiva 1985). In some predator-prey systems and for some types of nonrandom foraging, however, mathematical analysis of actual predator movements is both possible and fruitful. We examine such a situation in this paper, developing a mechanistic model of a spatially distributed interaction in which a predator's nonrandom foraging is characterized explicitly, and its effects subsequently quantified. The utility of this approach is that observations of how an individual predator searches can be translated into predictions about the ability of swarms of such predators to control particular prey (pest) populations or incipient outbreaks of prey.

The nonrandom foraging that concerns us here is "area-restricted search," or the widespread tendency of predators to restrict their foraging attention to the vicinity of recent captures before continuing a wider-ranging exploration. Examples are numerous and include coccinellids (Banks 1957), syrphids (Chandler 1969), blackbirds and thrushes (Smith 1971), neuropterans (Fleschner 1950), and even houseflies "preying on" sugar droplets (Murdie and Hassell 1973). Search-

Am. Nat. 1987. Vol. 130, pp. 233–270.

area restriction is typically achieved as a consequence of the predator's increasing frequency of directional changes immediately after finding and eating a victim (Curio 1976; Hassell 1978); reductions in the velocity of movement are also common (Hassell 1978). Our interest in area-restricted search evolved from a population-level study of a predator-prey interaction between the ladybug beetle, *Coccinella septempunctata*, and the goldenrod aphid, *Uroleucon nigrotuberculatum*. Field experiments have suggested that *Coccinella* can hold *Uroleucon* at low densities as long as ladybug foraging is unhampered (Kareiva 1985). Aggregation of *Coccinella* at incipient aphid outbreaks seems to be crucial to the control of aphids at these low densities (Kareiva 1984, 1985). Like most ladybugs, *Coccinella* beetles clearly exhibit area-restricted search behavior following the consumption of aphids (pers. obs.; Nakamuta 1985). We are interested in relating the details of *Coccinella*'s area-restricted search behavior to its aggregation at patches of high prey density and ultimately to its effectiveness as a regulator of aphid population growth. The models and analysis we present have application well beyond the *Coccinella-Uroleucon* interaction that stimulated our interest. Ideas in this paper extend to any predator that engages in area-restricted search, an enormous set in terms of the number and diversity of organisms.

This paper has many goals, including the advocacy of a mechanistic approach to nonrandom foraging models, a demonstration that area-restricted search does yield predator aggregation and an explanation of the precise reason for this, an exploration of the consequences of area-restricted search for predator-prey dynamics, an illustration of how observations of individual predator behavior can build to a population model of spatially heterogeneous predator-prey interactions, and a suggestion of what behavioral traits would predispose a predator toward being an effective biocontrol agent. To meet these goals, we switch between general abstract mathematical models, specific detailed models, reports of field experiments, and the analyses and "fit" of models to field data.

To put our theoretical efforts into context, we begin by briefly reviewing classical models, formulated as partial differential equations, of spatially varying dispersal. We then develop our own model of nonrandom population dispersal and aggregation, in which the key idea is that predators engage in area-restricted search. The derivation is lengthy because we take care to show how the macroscopic model follows from microscale observations of individual foraging predators. We discuss both an abstract model (for generality) and a specialized version of the model tailored to *Coccinella* to illustrate a concrete application. This juxtaposition of general and particular models is used throughout the paper. Once we have macroscopic population equations that can be derived from area-restricted search behavior, we discuss their interpretation and implementation in field situations. This leads to an actual application of the model to spatially distributed interactions between *Coccinella* and *Uroleucon*. In the application section, we describe field experiments and their results, and we fit our "special case" model to field data. Finally, we conclude by discussing some implications of our work for theories of biological control and for general ideas about spatially distributed predation systems.

CONTINUUM MODELS OF MOVEMENT CAN ACCOUNT FOR AGGREGATION

The movement of swarms of organisms has long been recognized as an important factor in population biology. Not surprisingly, then, numerous mathematical models have been developed to describe how the movements of each individual collectively influence the densities and spatial distributions of organisms (Okubo 1980). Continuum or partial-differential-equation dispersal models, which simultaneously track population changes in space and time, have been especially useful in ecology and population genetics (see review in Levin 1981). The classical applications of these models have involved diffusion or reaction-diffusion equations in which organisms are assumed to move randomly at rates that do not vary at different positions (Fisher 1937; Skellam 1951; Broadbert and Kendall 1953). Moreover, there have been extensive analyses of more biologically realistic models in which the rates at which organisms move vary in space (Okubo 1980); the density of conspecifics alters the rate of movement (Namba 1980); and organisms orient toward some particular chemical stimuli (Keller and Segel 1971; Segel 1984).

Pertinent to this paper's emphasis on predator aggregation are several continuum models that produce aggregations of organisms. We did not use any of these preexisting models because our interest was not in aggregation as an assumed result, but in working out mathematically the population-level consequences of area-restricted search. That is, we want to be able to convert measurements of the area-restricted search behavior exhibited by individual insects into a continuum model of spatially heterogeneous predator-prey interactions. With this approach, we obtain a computational procedure for forecasting complex changes in the macroscopic swarm behavior that different species of predators exhibit as a consequence of subtle changes in species-specific searching behavior.

Indeed, the equation we derive is somewhat similar to the taxis or aggregation equations that others have obtained by different methods. Probably the simplest continuum model capable of generating aggregation is

$$\partial P/\partial t = \partial^2[D(x)P]/\partial x^2 , \tag{1}$$

where $P(x, t)$ is the density of organisms at position x at time t, and D is a diffusion coefficient that varies along the spatial axis x. This can be derived as a special limiting case of a discrete random walk in which the probability of departure from a particular point, say x_n, depends only on the conditions at that point and not on conditions at x_{n-1} or x_{n+1} (see Okubo 1980 for this derivation). Equation (1) leads to a distribution of organisms that is aggregated in the regions on the x-axis where the diffusion (or motility) is lowest. As t approaches infinity, $P(x, t)$ approaches some constant divided by $D(x)$.

If one did not want to ground a model in the details of behavior, predator aggregation could be modeled conveniently by choosing a function for diffusion in equation (1) that represents declining predator mobility with increasing prey density. That is, let $D = D[V(x)]$, with $dD/dV < 0$, where $V(x)$ represents the spatially varying density of prey organisms. Later in the paper, we compare the equation we derive from the area-restricted search behavior with equation (1).

Even though it provides a ready and analytically simple characterization of predator aggregation, equation (1) should not be used to model the area-restricted searching we wish to study because hungry ladybug predators travel persistently along straight paths meters long and change direction only occasionally. The probability that such a path occurs as a consequence of many small steps made in the same direction is vanishingly small (in the kind of random-walk models described in Okubo 1980 that lead to eq. 1). Using a step length in a random-walk model equal to a typical long foraging run could explain such long "steps," but it would not lead to a continuum model that characterizes spatial patterns on scales less than a meter (and these small scales are important in *Coccinella*-aphid systems). As shown by Okubo, when random-walk models are extended to account for correlation among successive steps, then, instead of equation (1), the "telegraph equation" results (see Okubo 1980, eq. 5.17).

In our derivation, we assume that the natural state of each predator is one of persistent motion, punctuated occasionally by directional changes (and we obtain a system of equations closer to the telegraph equation than to eq. 1). Just the opposite assumptions are made in the random-walk models that lead to equation (1): the natural state of each predator is stationary, punctuated by occasional jumps. We believe that it is more important for the continuum model to account reliably for the underlying microscale behavior than to be analytically simple at the macroscopic level. There is a vigorous debate about what forms of a continuum model most naturally represent an organism whose movement is random but spatially varying, and thus biased. (Excellent discussions of these general issues can be found in Lauffenberger and Aris 1979; Alt 1980; Lapidus 1980; Segel 1984.)

THREE EXPERIMENTALLY MEASURABLE RESPONSE FUNCTIONS MODEL AREA-RESTRICTED SEARCH

We now express mathematically a widely held belief about how insects, lacking long-distance sensory perception, can find prey that are concentrated in some regions and sparse in others. The intuitive idea, abstracted from many diverse experimental observations (see, e.g., Murdie and Hassell 1973; Hassell and May 1974; Carter and Dixon 1982, 1984), is that each predator moves in a zig-zag trajectory, changing direction at a frequency that increases each time the predator eats a victim. This results in area-restricted search, as the term is usually understood.

One decision algorithm that could smoothly and simply determine a zig-zag frequency according to prey density would involve a predator whose turning rate depends on gut fullness. In particular, we might expect starving predators to move long distances in randomly chosen directions, and satiated predators to zig-zag to excess. This is exactly the behavior that is often observed (Curio 1976). Furthermore, this behavior does not require any special mental prowess; it requires only that something like the stretch receptors in an insect's gut can influence locomotion, an eminently plausible hypothesis.

We introduce a dimensionless variable, S, to measure the degree to which a

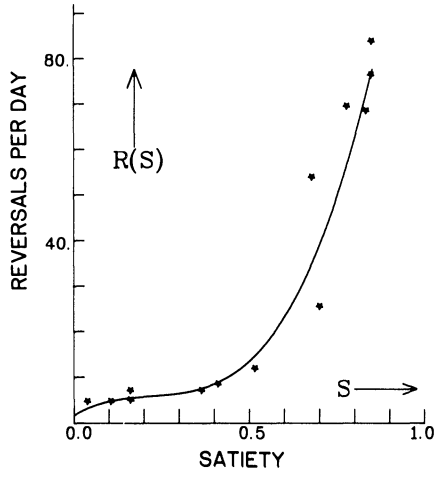

FIG. 1.—The predator direction-reversal frequency (number of turns per day), denoted by $R(S)$, is assumed to be a monotonically increasing function of gut satiety, S. The curve shown is the best fit to experimental data that we achieved in our study of *Coccinella-Uroleucon* interaction. *Stars*, Our measured-reversal data, given in table 2. Both ordinate and abscissa scales are linear.

predator is satiated. The minimum value of S is 0, which occurs when the predator has a totally empty digestive tract and is, by our definition, at its hungriest. The maximum value of S is 1, which occurs when the predator is satiated to the extent that it can consume no prey for lack of space in its digestive tract, although, even when $S = 1$, predators could continue to slaughter prey without consuming them.

Let u denote the speed at which a predator travels. We assume that u is constant for simplicity's sake. In fact, predators may temporarily cease all foraging activities to attend to other tasks (mating, grooming, etc.). Rather than thinking of these individuals as sedentary foragers, we view them as non-foragers that temporarily play no part in the predator-prey interaction we model. Let r denote the probability that a given predator changes direction during an interval of time, and assume that r is a function only of S:

$$r = R(S) , \tag{2}$$

in which we assume that the function R is smooth, monotonic, and increasing, as indicated qualitatively in figure 1.

Predator's Satiation Depends on the Prey Density Surrounding It during the Recent Past

S varies with time t, increasing each time the predator consumes a victim and decreasing as the predator digests and excretes. The predation rate must depend on the prey density experienced by the predator, $V(t)$, and on $S(t)$, since stomach fullness clearly influences a predator's inclination toward further predation. The rate of digestion, which is the rate at which $S(t)$ decreases in the absence of

feeding, must likewise depend on S. Thus, without having to know the habits peculiar to any particular insect species, we can assume the existence of a function $f(S, V)$ that determines the satiation of each predator according to the differential equation

$$dS/dt = f(S, V) . \tag{3}$$

We require $f(S, V)$ to be a smooth function and to satisfy two conditions that are essential to make equation (3) biologically sensible; namely,

$$\partial f/\partial S < 0 , \tag{4}$$

and

$$\partial f/\partial V \geq 0 . \tag{5}$$

Since $f(S, V)$ is the rate at which gut fullness increases, equation (4) means that, at every prey density, increments in gut fullness decrease the rate at which the gut fills. Equation (5) means that, at any fixed satiety, increasing the surrounding prey density never decreases the rate at which the gut fills. It is difficult to imagine violation of these conditions.

The mathematical consequences of equations (4) and (5) are crucial to a successful conclusion of this study. When the prey density is held constant, the steady-state solutions to equation (3) are the values of S that satisfy $f(S, V) = 0$. Equation (4) is precisely the condition needed by the implicit-function theorem to ensure that $f(S, V) = 0$ can be solved for S as a function of V and that, therefore, for each V, one and only one value of S solves that steady-state condition. We denote this steady-state value of S by

$$S = S_0(V) . \tag{6}$$

$S_0(V)$ is the solution that should be observed in predators that forage in a fixed constant-prey density, V, for a long time. When V is held fixed at any value, condition (4) means that equation (3) has a unique steady-state solution — namely, $S_0(V)$ — and that as t approaches infinity, S approaches $S_0(V)$. $S_0(V)$ is defined such that $f[S_0(V), V] = 0$.

Below, we need the fact that

$$dS_0/dV \geq 0 . \tag{7}$$

The biological interpretation of this is simply that, when V is held fixed, the equilibrium fullness of the predator's gut should be larger for larger values of V (prey density). This could hardly be otherwise. Intuition aside, condition (7) is a rigorous consequence of hypotheses (4) and (5).

We also wish to account for the commonly observed tendency of starving predators to consume a larger portion of each victim killed than a sated predator does (see, e.g., Cook and Cockrell 1978; Sih 1980). In our model, we denote the fraction (between 0 and 1) that a predator consumes of each victim killed by $\phi(S)$. We assume that ϕ is a monotonically decreasing function of S.

We need an expression, $K(S, V)$, for the number of prey organisms killed per unit of time per predator. To obtain $K(S, V)$, we note that $f(S, V)$ in equation (3)

must be the difference between a predator's consumption rate, $C(S, V)$, and its excretion rate, $E(S)$. That is, equation (3) should be expanded to

$$dS/dt = C(S, V) - E(S) \equiv f(S, V) . \tag{8}$$

We must also include in $C(S, V)$ a measure, α, of the conversion of partially consumed victims into "satiation," S. The parameter α is the number of victims that would satiate a starved predator if eaten entirely and quickly (before any digestion occurs). These definitions of α and $\phi(S)$ yield

$$C(S, V) = \phi(S)K(S, V)/\alpha , \tag{9}$$

with which equation (8) becomes

$$dS/dt = \phi(S)K(S, V)/\alpha - E(S) . \tag{10}$$

The variables r, K, and ϕ are directly observable experimentally. $E(S)$ and α, and thence $f(S, V)$, must be derived indirectly. As we show below, for a fixed spatial distribution of prey, the aggregation response of a swarm of predators is influenced only by the function $f(S, V)$ and is independent of how α, $\phi(S)$, $K(S, V)$, and $E(S)$ combine to constitute $f(S, V)$. The function $K(S, V)$ is important only in assessing the effect predation has in reshaping the prey distribution.

We have now defined three mathematical functions, $R(S)$, $f(S, V)$, and $K(S, V)$, that completely describe how predator searching and predation behavior change with prey density as a result of changes in the predator's gut fullness.

A Simple Explicit Example of the Predator Consumption-Digestion Function Illustrates the Practical Application of Our Model

To show how this general model can be applied in a specific instance, we give an example of the kind of function that $f(S, V)$ is likely to be. We use as a predator's consumption rate

$$C(S, V) = \gamma(1 - S)V/(1 + V/\nu) ; \tag{11}$$

and we use for a predator's excretion rate

$$E(S) = \lambda S , \tag{12}$$

where γ, ν, and λ are parameters. Thus, equation (8) becomes

$$dS/dt = f(S, V) = \gamma(1 - S)V/(1 + V/\nu) - \lambda S . \tag{13}$$

In this special illustrative case, the digestion (excretion) rate, given by the second term, is proportional to the amount held in the digestive tract. The rate at which predators fill up on prey is proportional to the remaining capacity of the digestive tract, $1 - S$, times a saturating function of prey density. This gives equation (13) two mechanisms for limiting the feeding rate as V increases. The $V/(1 + V/\nu)$ factor saturates at a maximum value of ν as V becomes large. In addition, regardless of the value of ν, large values of V in equation (13) lead to full stomachs ($S \approx 1$) and thus limitation of the feeding rate because of the $(1 - S)$ factor.

We use the simplest imaginable functional form for the fraction of each victim consumed, $\phi(S)$:

$$\phi(S) = 1 - \eta S , \tag{14}$$

in which $0 < \eta < 1$. Thus, from equation (9) we have the prey kill rate per predator:

$$K(S, V) = \frac{\alpha C(S, V)}{\phi(S)} = \frac{\alpha\gamma V(1 - S)}{(1 + V/\nu)(1 - \eta S)} . \tag{15}$$

From equation (13), we have

$$\partial f/\partial S = -\{\lambda + [\gamma V/(1 + V/\nu)]\} < 0 , \tag{16}$$

which confirms condition (4). Since $0 < S < 1$, condition (5) is confirmed by

$$\partial f/\partial V = \gamma(1 - S)/(1 + V/\nu)^2 \geq 0 . \tag{17}$$

For our illustrative case, we have

$$S_0(V) = \gamma V/[\lambda + V(\gamma + \lambda/\nu)] , \tag{18}$$

a saturating function of V. Finally, to confirm condition (7), we compute

$$dS_0/dV = \gamma\lambda/[\lambda + V(\gamma + \lambda/\nu)]^2 \geq 0 . \tag{19}$$

When victim density is constant and S approaches $S_0(V)$, then equation (18) substituted into equation (15) yields a type-II functional response (Holling 1965) of predators to prey density: the per-predator kill rate at equilibrium is

$$K[S_0(V), V] = \frac{\alpha\gamma V}{1 + [\gamma(1 - \eta)/\lambda + 1/\nu]V} . \tag{20}$$

Our derivation now proceeds using the general function $f(S, V)$, but we return to this special case later to illustrate a concrete application.

SIMPLE ASSUMPTIONS CONCERNING MICROSCALE BEHAVIOR YIELD A PREDATOR-FLUX CONSTITUTIVE EQUATION

Average Predator Flux Depends on the Direction-Reversal Frequency

In this section, we build on a previous analysis (Segel 1977) concerning the chemotactic pursuit of chemical nutrients by *Escherichia coli* bacteria, which exhibit the same zig-zag trajectories typical of insect predators and a similar modulation of their turning frequency as a function of recent food encounters. (For citations of the relevant bacterial chemotaxis literature, see Segel 1977.)

For simplicity, we restrict attention to the case of predators traversing a one-dimensional domain. They move at a fixed speed u and must, at each time, be progressing either left or right. The variable x measures displacement in this one-dimensional space. At each instant t and at each position x, the total population of predators can be partitioned into two subsets: those moving to the right, and those moving to the left. We use "$\Rightarrow$" superscripts to represent the right-

moving predators and "$\Leftarrow$" superscripts to represent the left-moving predators. Let $n^{\Rightarrow}(x, t)$ be the number density of predators moving to the right at (x, t); $n^{\Leftarrow}(x, t)$, the number density of predators moving to the left at (x, t); $r^{\Rightarrow}(x, t)$, the direction-reversal probability per unit of time for predators moving to the right at (x, t); and $r^{\Leftarrow}(x, t)$, the direction-reversal probability per unit of time for predators moving to the left at (x, t).

Since right-moving predators move at velocity u and left-moving ones move at velocity $-u$, we obtain the following conservation laws for $n^{\Rightarrow}$ and $n^{\Leftarrow}$ (see Segel 1977).

$$\partial n^{\Rightarrow}/\partial t + u\,\partial n^{\Rightarrow}/\partial x = r^{\Leftarrow}n^{\Leftarrow} - r^{\Rightarrow}n^{\Rightarrow}\,, \tag{21}$$

$$\partial n^{\Leftarrow}/\partial t - u\,\partial n^{\Leftarrow}/\partial x = -(r^{\Leftarrow}n^{\Leftarrow} - r^{\Rightarrow}n^{\Rightarrow})\,. \tag{22}$$

Equations (21) and (22) are valid regardless of the mechanism by which $r^{\Rightarrow}$ and $r^{\Leftarrow}$ are determined. Thus, we first assume that $r^{\Rightarrow}$ and $r^{\Leftarrow}$ are somehow prescribed and determine the consequences these reversal probabilities have on the predator population's average flux density. Then, we connect $r^{\Rightarrow}$ and $r^{\Leftarrow}$ to the satiety of right-moving and left-moving predators through equations (2) and (3).

The density of predators at (x, t), which include both left-moving and right-moving subpopulations, is

$$P(x, t) = n^{\Rightarrow} + n^{\Leftarrow}\,, \tag{23}$$

and the flux density of predators (defined as the rate at which predators cross, in the positive x direction, a unit of area that is oriented perpendicular to the x-axis) is

$$J_P = u(n^{\Rightarrow} - n^{\Leftarrow})\,. \tag{24}$$

Adding equations (21) and (22) and using equations (23) and (24), we obtain the usual conservation equation for P:

$$\partial P/\partial t = -\partial J_P/\partial x\,. \tag{25}$$

Now, subtracting equation (22) from equation (21), multiplying by u, and using the inverse of equations (23) and (24), we find

$$n^{\Rightarrow} = (P + J_P/u)/2 \tag{26}$$

and

$$n^{\Leftarrow} = (P - J_P/u)/2\,. \tag{27}$$

This leads to the equation for determining the predator flux density:

$$\partial J_P/\partial t + u^2\,\partial P/\partial x = -J_P(r^{\Rightarrow} + r^{\Leftarrow}) + uP(r^{\Leftarrow} - r^{\Rightarrow})\,. \tag{28}$$

Unfortunately, equation (28) is a partial differential equation for the predator flux density, J_P, rather than a direct algebraic relationship specifying J_P. Although we could use equation (28) in a continuum population model when computing solutions numerically, we feel that it is better to make an algebraic approximation of J_P since it will be easier to understand our model and to examine its dynamic

behavior if we can specify J_P directly. We assume that when predator individuals experience a gradually changing environment (i.e., varying prey and predator densities), they "quickly" adjust their movement behavior (i.e., the direction-reversal probabilities) to what it would be had they always been in the same local environment. That is, we assume that the solution, J_P, to equation (28) relaxes "instantaneously" to the same steady state found by allowing t to approach infinity.

The words *quickly* and *instantaneously* mean that changes in the movement behavior of predators are assumed to occur much more rapidly than changes in the predator's or prey's spatial distributions. This is the case if, during a characteristic time needed for a significant alteration of population distribution, each predator changes direction several times, an experimentally verifiable assumption.

The quasi-static equilibrium approximation described in the preceding paragraph is implemented simply by setting the time derivative in equation (28), $\partial J_P/\partial t$, to zero. This does not mean that $\partial J_P/\partial t$ is small; rather, if the other terms in the equation ever fail to balance each other, then the $\partial J_P/\partial t$ term can become as large as may be required to equilibrate the other terms instantaneously. When we do this, equation (28) becomes an algebraic equation easily solved for the flux density, J_P:

$$J_P = -\left(\frac{u^2}{r^{\Leftarrow} + r^{\Rightarrow}}\right)\frac{\partial P}{\partial x} + P\left(\frac{r^{\Leftarrow} - r^{\Rightarrow}}{r^{\Leftarrow} + r^{\Rightarrow}}\right)u\,. \tag{29}$$

Equation (29) expresses the number of predators per unit of time per unit of area passing a particular point as a function of the predator's spatial distribution, velocity, and turning frequencies.

Deriving the Reversal Probabilities from Assumed Microscale Behavior Yields a Specific Flux Constitutive Equation

Since the mathematical analysis needed to estimate $r^{\Leftarrow}$ and $r^{\Rightarrow}$ is not transparent, we provide an intuitive description of the expected result and then banish to Appendix A most of the technical details involved in its derivation.

Suppose a fixed spatial gradient in density of prey, $V(x)$, were imposed, increasing to the right (that is, $\partial V/\partial x > 0$), and that predators distributed uniformly throughout the domain were forced to remain motionless. Then according to conditions (3), (4), and (5), S would relax to the equilibrium satiety given in equation (6): $S(x) \to S_0[V(x)]$. Because of condition (7), this $S(x)$ would be a monotonic, increasing function of x. Figure 2 shows a qualitative graph of $V(x)$ and $S_0[V(x)]$ under these "thought experiment" conditions.

Once the $S_0[V(x)]$ equilibrium profile has been reached, when the previously immobilized predators are released, they begin moving, either right or left, at speed u. Right-moving predators arriving at a particular location, x^*, have come from a position left of x^* at which $S < S_0[V(x^*)]$ and have moved through territory in which that inequality holds. While they move, their gut fullness relaxes (via eq. 22) toward the ever-increasing values of $S_0[V(x)]$ they see. But the S value of right-

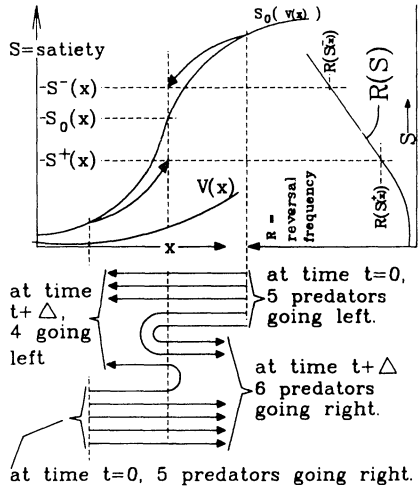

FIG. 2.—The upper left plot shows an assumed prey gradient, $V(x)$, and the corresponding gut satiety, $S_0[V(x)]$, that motionless predators would have when equilibrated to the prey density, $V(x)$, at x. Suppose that an initially (and artificially motionless) distribution of equilibrated predators is suddenly freed to migrate. Initially, half of the predators move to the right, and the other half move to the left. Left-moving predators arriving at x have traveled through territory with higher prey densities than they find at x. They arrive at x, therefore, with a fuller gut, $S^{\Leftarrow}(x)$, than they would have if they had always been at x. A symmetrical argument shows right-moving predators arrive at x with $S^{\Rightarrow}(x) < S_0(x)$. These arguments depend only on $S_0(V)$'s being a monotonically increasing function of V. In the upper right plot, rotated 90°, the reversal frequency, $R(S)$, is graphed to show why left-moving predators arrive at x with a higher reversal probability than do right-moving predators. That is, $R[S^{\Leftarrow}(x)] > R[S^{\Rightarrow}(x)]$. The lower half of the figure illustrates schematically how our theory of area-restricted search leads to a preytactic flux of predators up the prey gradient. Because of their higher reversal frequency, only three of the five left-moving predators continue moving left as they reach position x; two reverse. Four of the five right-moving predators continue moving past x to the right. Thus, near x, after a short time, D, six predators are moving to the right and four to the left, yielding a net flux of two to the right toward the higher prey concentration.

moving predators, denoted by $S^{\Rightarrow}$, is always slightly less than $S_0[V(x)]$. $S^{\Rightarrow}(x^*)$ therefore is less than $S_0[V(x^*)]$. For reasons of symmetry, $S^{\Leftarrow}(x^*)$—the satiety measure of left-moving predators arriving at x^*—exceeds $S_0[V(x^*)]$. This is shown schematically in figure 2.

Clearly then, with $r^{\Rightarrow} = R(S^{\Rightarrow})$ and $r^{\Leftarrow} = R(S^{\Leftarrow})$, when $R(S)$ is an increasing function of gut fullness or satiety, we have, as a consequence of

$$S^{\Rightarrow}(x^*) < S_0[V(x^*)] < S^{\Leftarrow}(x^*) , \tag{30}$$

$$r^{\Leftarrow} > r^{\Rightarrow} . \tag{31}$$

This means that the second term in equation (29) is positive whenever $\partial V/\partial x > 0$. Steepening the imposed gradient of $V(x)$ should amplify the difference $r^{\Leftarrow} - r^{\Rightarrow}$; intuitively, then, we expect that

$$r^{\Leftarrow} - r^{\Rightarrow} \propto \partial V/\partial x . \tag{32}$$

As shown in the more precise analysis that follows, the second term of equation (29) thus corresponds to the taxis of predators in the direction of the gradient of prey density, at a speed proportional to that gradient's amplitude. This, intuitively, is the mechanism by which area-restricted search is equivalent to "prey-taxis," or movement toward clusters of prey.

To transform the preceding prose into explicit formulas and thus connect the general expression (29) for predator flux to the microscale behavior, we proceed to write conservation equations for the quantities $S^{\Rightarrow}$ and $S^{\Leftarrow}$. These are analogous to equations (21) and (22) but involve the local S dynamics specified in equation (3):

$$\partial(n^{\Rightarrow}S^{\Rightarrow})/\partial t + u\,\partial(n^{\Rightarrow}S^{\Rightarrow})/\partial x = r^{\Leftarrow}n^{\Leftarrow}S^{\Leftarrow} - r^{\Rightarrow}n^{\Rightarrow}S^{\Rightarrow} + n^{\Rightarrow}f(S^{\Rightarrow}, V)\,, \quad (33)$$

$$\partial(n^{\Leftarrow}S^{\Leftarrow})/\partial t - u\,\partial(n^{\Leftarrow}S^{\Leftarrow})/\partial x = -r^{\Leftarrow}n^{\Leftarrow}S^{\Leftarrow} + r^{\Rightarrow}n^{\Rightarrow}S^{\Rightarrow} + n^{\Leftarrow}f(S^{\Leftarrow}, V)\,. \quad (34)$$

When equations (21) and (22) are used to simplify the left-hand side of these two equations, we obtain

$$\partial S^{\Rightarrow}/\partial t + u\,\partial S^{\Rightarrow}/\partial x = -(r^{\Leftarrow}n^{\Leftarrow}/n^{\Rightarrow})(S^{\Rightarrow} - S^{\Leftarrow}) + f(S^{\Rightarrow}, V)\,, \quad (35)$$

$$\partial S^{\Leftarrow}/\partial t - u\,\partial S^{\Leftarrow}/\partial x = (r^{\Rightarrow}n^{\Rightarrow}/n^{\Leftarrow})(S^{\Rightarrow} - S^{\Leftarrow}) + f(S^{\Leftarrow}, V)\,. \quad (36)$$

We now consider a special circumstance in which a gradient in $V(x)$ is imposed and held constant in time. We suppose further that some predators are allowed to wander on this V gradient. Finally, we suppose that, initially at least, the gradient $\partial P/\partial x$ remains small (i.e., the few predators are uniformly distributed). When these artificial but revealing circumstances exist and when other mild conditions are met, then we can collapse the set of three partial differential equations (3), (35), and (36), plus the algebraic reversal-probability equation (2) to two single algebraic relationships. This is done in Appendix A, and the results are

$$r^{\Leftarrow} - r^{\Rightarrow} = \left(2u\,\frac{dR}{dS}[S_0(V)]\,\frac{dS_0}{dV}(V)\Big/\left\{2R[S_0(V)] - \frac{\partial f}{\partial S}\,[S_0(V), V]\right\}\right)\frac{\partial V}{\partial x}\,, \quad (37)$$

$$r^{\Leftarrow} + r^{\Rightarrow} = 2R[S_0(V)]\,. \quad (38)$$

Substituting equations (37) and (38) into equation (29) yields

$$J_P = -\left\{\frac{u^2}{2R[S_0(V)]}\right\}\frac{\partial P}{\partial x} + P\left(\frac{u^2\,\frac{dR}{dS}[S_0(V)]\frac{dS_0}{dV}(V)}{R[S_0(V)]\left\{2R[S_0(V)] - \frac{\partial f}{\partial S}\,[S_0(V), V]\right\}}\right)\frac{\partial V}{\partial x}\,. \quad (39)$$

Equation (39) is our main result. Notice that, given local values of $P(x, t)$ and $V(x, t)$, every factor of every term in equation (39) can be computed explicitly from u and the two functions $R(S)$ and $f(S, V)$, all of which can be obtained by observing the foraging behavior of individual predators; there is no phenomenology here. Although equation (39) is an algebraically complicated recipe, it nevertheless serves as a direct, computationally tractable, transformation rule. It con-

verts microscale behavioral data into the population-level rule needed for a continuum model of predators aggregating at prey clusters as a consequence of area-restricted search.

THE FLUX EQUATION FOR PREDATORS GENERATES PREYTAXIS

Flux Represents a Superposition of Random Dispersion and Directed Preytactic Pursuit

In equation (39), we obtained a particular version of a general constitutive equation for the flux of self-propelled organisms, proposed originally by Keller and Segel (1970) and adapted by them to account for traveling bands of *Escherichia coli* bacteria (Keller and Segel 1971). These bacteria move chemotactically up the gradient of a chemical substrate that they consume and whose concentration gradient they thus deform. We obtained equation (39) using an approach first suggested by Segel (1977). A substantial literature has sprung from Keller and Segel's original paper. This chemotaxis literature may contain valuable information for population biologists since, as we have just shown, area-restricted search behavior of arthropod predators leads to a constitutive equation for flux closely resembling the equation on which this theoretical chemotaxis literature is founded. We name the terms in equation (39) following the nomenclature introduced by Keller and Segel to facilitate connection with that literature. (For papers with extensive bibliographies of this literature, see Segel 1984.)

Keller and Segel asserted the following phenomenological constitutive equation for the flux of chemotactically active organisms:

$$J_P = -D_P(V)\partial P/\partial x + P\chi(V)\partial V/\partial x . \tag{40}$$

They called D_P the *random-motility coefficient*, which they took to be a constant for simplicity of analysis. Keller and Segel called $\chi(V)$ the *chemotactic-sensitivity coefficient* (and they used the functional form $\chi(V) = \delta/V$). The diffusive contribution to flux (the first term on the right-hand side of eq. 40) causes attenuation of predator concentration peaks regardless of how $D_P(V)$ varies with V. Comparing equations (39) and (40), we see that the analogous random-motility coefficient appropriate for area-restricted search is

$$D_P(V) = u^2/2R[S_0(V)] . \tag{41}$$

This expression for random motility makes intuitive sense: this diffusion coefficient increases as the square of the speed at which predators travel; faster travel means more-rapid dispersal. The denominator is the direction-reversal probability of predators if their gut equilibrates to the satiety corresponding to a prey density of V. As V increases, this reversal probability also increases and diminishes the diffusion coefficient; more food inhibits dispersal.

By comparing equations (39) and (40), we identify the *preytactic* (as opposed to *chemotactic*) sensitivity coefficient appropriate for area-restricted search as

$$\chi(V) = u^2 \frac{dR}{dS}[S_0(V)]\frac{dS_0}{dV}(V) \Big/ \left(R[S_0(V)]\left\{2R[S_0(V)] - \frac{\partial f}{\partial S}[S_0(V), V]\right\}\right) . \tag{42}$$

Equation (42) is somewhat more difficult to interpret intuitively. In general, the last term of equation (40) means that predators move up the concentration gradient of the food they seek at an average speed of $\chi(V)\partial V/\partial x$; $\chi(V)$ measures the sensitivity of this taxis per unit of strength of the gradient, $\partial V/\partial x$. One obtains the net predator flux up the V gradient by multiplying this average speed by the predator density at the point in question.

The u^2 term in the numerator of equation (42) means that faster-moving predators "chase" their prey faster if other effects remain constant. By the chain rule of differential calculus, the rest of the numerator in equation (42) is

$$d\,R[S_0(V)]/dV\,. \tag{43}$$

This is the rate of increase of the reversal probability per unit of increase in prey density. Since it is the modulation of directional change by changes in prey density that gives rise to taxis, the numerator makes intuitive sense. Condition (7) means that the numerator in equation (42) is positive.

The denominator of equation (42) is intuitively obscure, at least to us. Note that condition (4) guarantees that the term enclosed in the braces cannot vanish or become negative. The denominator of equation (42) increases as V increases because of the assumed monotonicity of the function $R(S)$ and because of condition (7). Roughly speaking, the denominator of equation (42) causes $\chi(V)$ to increase as the prey density decreases. The biological interpretation is that predators become more sensitive to gradients in prey density as the prey density falls toward zero; starving predators seek prey more actively than satiated ones do.

Earlier, we introduced equation (1) as a model that arises from taking limits of discrete random walks in which the probability of departing from a point depends on conditions at that point. By rewriting equation (1) so that that departure probability depends on the prey density at each point, $V(x)$, we can compare this simpler result with our area-restricted-search result (eq. 39). According to equation (1), the predator flux density is given by

$$J_P = -\partial[D(V)P]/\partial x = -(P\,dD/dV)\partial V/\partial x - \{D[V(x)]\}\partial P/\partial x\,. \tag{44}$$

Equation (44) somewhat resembles equation (39). Indeed, if, through measurement, $\partial f/\partial S$ always turned out to be zero, then, using the substitution

$$D(V) \equiv u^2/2R[S_0(V)]\,, \tag{45}$$

the result of an area-restricted search (eq. 39) and the more easily derived result for a random walk (eq. 44) would be identical. This suggests that equation (39) can be viewed as a generalization of the random-walk aggregation models of equation (1); equation (39) approaches equation (44) as $|\partial f/\partial S|$ approaches zero.

However, $\partial f/\partial S$ cannot equal zero because that would imply that the amount a predator eats has no effect on its predation rate. We know from direct observation of ladybug feeding that $|\partial f/\partial S|$ is far from zero; as ladybugs become satiated, their rate of consumption can fall to 10% or 1% of that of an "empty" or starved beetle (pers. obs. for *Coccinella*; the trend is probably common in many predators). This decrease in feeding rate with gut fullness is greatest for starved ladybugs and

diminishes as beetles approach satiation (i.e., as S approaches 1). In terms of a movement equation, it might be useful to think of $\partial f/\partial S$ as giving information about prey density that is not entirely local; the $\partial f/\partial S$ term in equation (42) represents a mechanism by which predators "remember" foraging conditions in a recently visited territory.

In the remainder of this paper, we use equation (39) to describe *Coccinella* foraging, both because it is the model that emerges from our area-restricted-search derivation and because we know that, in general, $\partial f/\partial S$ cannot be assumed to be close to zero.

For other applications, equation (44) may work just as well, and it is much simpler to use. However, if equation (44) were used without any derivation from first principles, then some method for estimating quantitatively how $D(V)$ varies with prey density would be needed. One possibility might be to observe how a swarm of predators changed its distribution through time (as opposed to observing individual behavior) and to apply a parameter-estimation algorithm to the spatio-temporal data (see Banks et al. 1985 for such an example).

The Predator Flux Equation Predicts Predator Aggregation at Prey Density Peaks

The practical utility of equation (39) is that it accounts for the net migration of the predator population. Some constitutive equation must be formulated for prey flux density, J_V, as well, to obtain a well-set theory. Even without specifying J_V, however, we can use equation (39) to obtain a useful description of the aggregation that results from area-restricted search.

Suppose that the net birth-death rate for predators is held to zero by experimental contrivance. Suppose further that a time-invariant, spatially heterogeneous distribution of prey density, $V(x)$, can be maintained and that a fixed number of predators is allowed to forage in the fixed prey distribution. We can then use equation (39) to predict the steady-state spatial distribution that the predator population should eventually approach. In effect, this gives us a means of testing our aggregation model; we can compare the observed steady state for $P(x)$ to that predicted by equation (39). In particular, the steady-state equilibrium distribution of predators is reached when the predator flux density is everywhere equal to the same constant, that is, when

$$J_P \equiv \text{constant} . \tag{46}$$

Suppose that our one-dimensional spatial domain over which predators can roam extends from $x = 0$ to $x = L$ and that by experimental contrivance the predators cannot escape (or enter) through the ends of this domain. (We are currently conducting greenhouse experiments that duplicate these conditions.) Then, the constant in equation (46) must be the zero value of predator flux at the boundaries. Using the shorthand notation of equation (40), this means

$$J_P = - D_P(V)\partial P/\partial x + P\chi(V)\partial V/\partial x = 0 , \tag{47}$$

so that

$$(dP/dx)/P = \{\chi[V(x)]/D_P[V(x)]\}\, dV(x)/dx . \tag{48}$$

Equation (48) can be solved explicitly. We obtain

$$P(x) = P_T B \exp\left(\int_{V(0)}^{V(x)} \frac{\chi(W)}{D_P(W)}\, dW\right), \tag{49}$$

where $P_T B$ is an integration constant. P_T denotes the total number of predators in the domain and the quantity in parentheses gives a normalized spatial predator-distribution profile. The value of the constant B is chosen to normalize the distribution so that the spatial integral of the quantity in parentheses is 1. The quantity in parentheses is analogous to a probability distribution.

From equations (41) and (42), the integrand in equation (49) is

$$\frac{\chi(V)}{D_P(V)} = \frac{2dR[S_0(V)]/dV}{2R[S_0(V)] - \partial f[S_0(V), V]/\partial S}. \tag{50}$$

Since equation (50) is not a simple integrand, the predator distribution predicted by equation (49) cannot be computed analytically. A numerical quadrature computer program can, however, easily calculate $P(x)$ given by equations (49) and (50) whenever the functions $R(S)$ and $f(S, V)$ have been determined by field data.

Later in this paper, we work through one realistic example using equation (49) and show how to relax the restriction that predators do not die or emigrate and still compute $P(x)$ when $V(x)$ does not change with time (see Appendix B).

Our Model Accounts for Both Flux and Source-Sink Population Dynamics

Processes other than local movement (or flux) contribute to density changes in natural populations of predators and prey. For instance, birth, death, emigration, and immigration may all be important.

The general partial differential equation that accounts collectively for all such spatiotemporal changes in a scalar quantity $Q(x, t)$ (such as heat, concentration of a chemical, or the population density of some organism) in one spatial dimension, x, is

$$\partial Q/\partial t = -\partial J_Q/\partial x + \sigma_Q, \tag{51}$$

where J_Q is the flux density of the quantity Q, and σ_Q is the creation-rate density (or net source term) of Q. To use this general scalar conservation equation to model the dynamics of any particular substance, we must assert expressions that determine how J_Q and σ_Q depend on $Q(x, t)$ and possibly other variables. These are called *constitutive equations*.

We need two copies of equation (51): one for the aphid prey, where Q stands for $V(x, t)$; and another for the ladybug predators, where Q stands for $P(x, t)$. Thus, we need constitutive equations for J_V, σ_V, J_P, and σ_P. The major theoretical contribution of this paper is to propose and justify equation (39) (or 40) as the appropriate constitutive equation for J_P when P represents predators that forage by area-restricted search.

We assume that aphids move randomly and that the constitutive equation for aphid flux density is

$$J_V = -D_V \partial V/\partial x. \tag{52}$$

The source term for aphids is the difference between net birth (σ_{Vn}) and death by predation (σ_{VK}):

$$\sigma_V = \sigma_{V\mathrm{n}}(V, P) - \sigma_{VK}(V, P), \tag{53}$$

where $\sigma_{V\mathrm{n}}$ and $\sigma_{V\mathrm{K}}$ are functions of local density.

The source term for predators is

$$\sigma_P = \sigma_{P\mathrm{a}}(V, P) - \sigma_{P\mathrm{d}}(V, P). \tag{54}$$

The first term on the right side accounts for predator immigration (by flight from remote locations), and the second term for predator emigration (by flight to remote locations). Note that *all* terms in the predator equation below (eq. 56) represent movements of predators. The flux term (from eq. 47) models continuous horizontal crawling along a one-dimensional hedge, and the σ_P terms model arrivals ($\sigma_{P\mathrm{a}}$) and departures ($\sigma_{P\mathrm{d}}$) by flight. In other predator-prey systems, the net σ_P term may involve predator birth or predator death. Substitution of equations (40), (52), (53), and (54) into the two copies of equation (51) yields our complete spatially distributed predator-prey model:

$$\partial V/\partial t = DV\partial^2 V/\partial x^2 + \sigma_{V\mathrm{n}}(V, P) - \sigma_{VK}(V, P), \tag{55}$$

and

$$\partial P/\partial t = (\partial/\partial x)[D_P(V)\partial P/\partial x - \chi(V)P\partial V/\partial x] + \sigma_{P\mathrm{a}}(V, P) - \sigma_{P\mathrm{d}}(V, P). \tag{56}$$

From equation (20), the rate at which aphids are killed by ladybugs is

$$\sigma_{VK}(V, P) = PK[S_0(V), V] = \alpha\gamma VP/\{1 + [\gamma(1 - \eta)/\lambda + 1/\nu]V\}. \tag{57}$$

We can now solve equations (55) and (56) numerically, which we do below in the context of a specific ladybug and aphid system.

EXPERIMENTAL DATA DETERMINE PARAMETERS IN THE PREDATOR PREYTAXIS MODEL

To characterize predator foraging according to equation (40), we use the specific-digestion differential equation (13) and an explicit parameterized formula for the reversal probability, $R(S)$. In general, we need data on the feeding rate as a function of satiation, which can be controlled by feeding predators until they are sated and then starving them for different lengths of time before observing their feeding in vegetation with a known prey density; the turning or reversal frequency as a function of satiation, which depends in turn on prey density; and the mean free-path velocity of searching predators.

Since satiation depends on local prey density, quantifying the effect of satiation allows us to characterize foraging as a function of spatially heterogeneous prey distributions. Many observations of individual predators, each lasting for 20–30 min, produce the raw data we need. By fitting these data to functions such as equation (20), we can completely specify a population model using individual behaviors as our input. We illustrate this approach with a specific study of the interaction between the ladybug *Coccinella septempunctata* and its aphid prey *Uroleucon nigrotuberculatum*.

The Model Is Tailored to Ladybugs' Preying on Aphids

Coccinella septempunctata is a voracious predator of aphids, which the U.S. Department of Agriculture has imported to North America as a biological control agent (Obrycki et al. 1982). Although it is a generalist, in our studies of *Coccinella*, *Uroleucon* constituted about 90% of its diet (Kareiva 1984). Since *Uroleucon* is confined to goldenrod, the interaction between *Coccinella* and *Uroleucon* can be studied by experimental contrivance (e.g., mowing and weeding) in simple environments of any desired geometry (Kareiva 1984, 1985). Our experiments were performed in uniform rows of goldenrod; these circumstances represent a field approximation to the mathematician's abstraction of a spatially distributed predator-prey interaction on a one-dimensional domain, exactly the situation described by equations (55) and (56). Ladybug populations are, however, far from homogeneous behaviorally; different instars of *Coccinella* feed and move at rates that differ by an order of magnitude. Adults are the most long-lived stage, and perhaps the most voracious. The 6 weeks of a Rhode Island summer during which adult *Coccinella* are abundant is also the period when the fate of aphid populations is largely determined. Further, by virtue of their mobility, adults are the stage in *Coccinella*'s life cycle with the strongest aggregating response.

Hence, as a first step, we focus here on a model for *Coccinella* adults alone. Because of this restriction, the model presented in this paper does not permit year-to-year predictions about predator-prey dynamics. The time scale of interest to us is the 4–6 wk of midsummer when aphid outbreaks appear, if they appear at all. We seek to understand how the area-restricted search of some given pool of *Coccinella* adults contributes to the possible control of incipient *Uroleucon* outbreaks. Although these are limited goals, they represent the scope required of theory pertaining to agroecosystems in general (Murdoch 1975) or biological control systems in particular (Murdoch et al. 1985). Year-to-year dynamics are less important because they are, in a sense, set by man, who provides new inputs into agroecosystems each growing season.

Two Kinds of Short-Term Foraging Experiments Are Needed

Our experiments to characterize *Coccinella* foraging were done with marked adults that were chilled and released early in the morning. Even so, some adults were disturbed and flew away. Other adults wandered out of our experimental areas (goldenrod rows) or were simply lost while we were following them. The data we report below are for undisturbed adults that were never lost and never left our experimental goldenrod rows. (If our experiments are to be repeated or applied to another species, many more individuals must be marked and released than actually end up contributing to the data.) We also restricted our experiments to warm sunny weather. Because temperature has a well-documented effect on ladybug foraging (Gutierrez et al. 1980), we sought to minimize this source of variation as much as possible. Obviously, it was not in our power to control the weather, and we believe that much of the variation evident in our data reflects the influence of temperature on foraging. Weather effects should not, however, bias our results in any particular direction.

To determine the five parameters γ, λ, ν, η, and α, which in equations (13) and (20) characterize ladybug killing and digestion of aphids, we performed two types of foraging experiments in July 1984 and in June and July 1985. First, we conducted what we call *starvation/satiation experiments*. The purpose of these experiments was to estimate the rate at which satiated ladybugs emptied their gut (or lost their sated feeling) in a manner that would be reflected in changing consumption rates. We fed certain ladybugs on a superabundance of aphids until satiation was observed. These satiated ladybugs were then starved for measured time intervals, denoted by τ, and subsequently observed foraging in the field along rows of goldenrod plants with known uniform aphid densities. We followed each ladybug individually, observing them continuously for 30 min and recording each aphid consumed. This was done for ladybugs representing six different τ's and a variety of aphid densities. All ladybugs were handled in the same fashion.

Our second experiment, which we call the *foraging-rule experiment*, consisted of observations of ladybug foraging in rows of goldenrod that had been manipulated to contain different spatially uniform densities of aphids. The focus of this experiment was the influence of prey density on ladybug foraging *trajectories*. Ladybugs were allowed to equilibrate their behavior to the density of aphids in our goldenrod rows for half of a day (this is enough time for S to reach an equilibrium with V). After that half-day (a morning), we followed individual ladybugs for 20-min observation bouts, observing the number of times each beetle reversed its direction of movement, how many aphids it ate, and the number of seconds it spent eating each aphid.

Initially, we did this experiment without recording the time each ladybug spent eating each aphid. We soon realized that eating time varied dramatically with prey density in a way that could be an important determinant of how many aphids a ladybug can eat in one day. In particular, as aphid density increases, ladybugs spend less time eating each aphid and apparently consume less and less of each aphid. When aphids are extremely dense, ladybugs seem to take just one big, juicy bite out of each aphid before moving to the next victim. This is the phenomenon that the function $\phi(S)$ accounts for and is the reason that the per-predator kill rate $K(S, V)$ exceeds the consumption rate $C(S, V)$ (see eq. 9). Such partial consumption of prey has been observed in many predatory insects (Sih 1980). Sih (1980) used optimal foraging theory to argue that, in general, as prey density increases, predators should consume ever-declining proportions of each prey item. Although here we do not attempt to explain the trend, it is clear that ladybugs eat less of each aphid (reflected by time spent feeding) at high aphid densities than at low aphid densities (see table 3, below).

The final parameter we estimate is the speed of the foraging ladybug. This speed is crucial because u is squared in both the random-motility coefficient (eq. 41) and the preytactic-sensitivity coefficient (eq. 42). Doubling the speed of a predator causes a fourfold increase in the rates of aggregation or dispersal. In comparisons of the aggregation efficacies of different species of predators, u is the most crucial behavioral parameter to measure.

There are several ways to measure u experimentally. One is to measure the total distance traveled by individually following ladybugs during observation times of

several hours each. Alternatively, standard "point-release" experiments suffice (see Kareiva 1982), and this is the approach we adopted. In early experiments (Kareiva 1984), the mean-squared dispersal distance, l^2, in a swarm of ladybugs one day after a point release in a goldenrod tract with a spatially uniform aphid population was measured. These releases were performed when the aphid densities were $V = 5$ aphids/m and $V = 50$ aphids/m.

A CONSTRAINED NONLINEAR PARAMETER-OPTIMIZATION ALGORITHM FITS THE PREYTAXIS MODEL TO FIELD DATA

Before fitting our model to the data, we must complete its mathematical specification by picking a parameterized recipe for $R(S)$, namely, the following third-degree polynomial:

$$R(S) = \beta_0 + \beta_1 S + \beta_2 S^2 + \beta_3 S^3 . \tag{58}$$

We must constrain the parameters $\{\beta_0, \beta_1, \beta_2, \beta_3\}$ such that $R(S)$ is a monotonically increasing function of S that corresponds to the graph in figure 1. Using this particular $R(S)$ function and equations (16), (18), (19), and (58), we can rewrite equations (41), (42), and (50) as explicit functions of V and of the parameter vector

$$\Gamma = (\eta, \gamma, \lambda, \nu, \alpha, \beta_0, \beta_1, \beta_2, \beta_3, u) . \tag{59}$$

Γ is an experimentally accessible parameter set, in which u is the speed at which an individual predator moves; η, γ, λ, ν, and α characterize predator killing, consumption, and digestion of prey; and β_0, β_1, β_2, and β_3 characterize predator direction-change statistics.

To fit our model to the data, our general strategy is to devise a function, $\Omega(\Gamma)$, that measures the amount by which the predictions made by equations (13) and (58), with a given parameter vector Γ, fail to fit our experimental data. An Ω equal to zero would mean a perfect fit; the larger Ω is, the worse the fit is. We seek the "best fit" value of $\Gamma = (\eta, \gamma, \lambda, \nu, \alpha, \beta_0, \beta_1, \beta_2, \beta_3, u)$ that corresponds to minimal values of Ω, using a constrained nonlinear parameter-optimization procedure called the *ellipsoid algorithm* (see Ecker and Kupferschmid 1985).

The explicit formulas that result from a numerical fit are too algebraically complicated to write down. The important concept is that our theory produces explicit recipes for the random-motility coefficient, $D_P(V, \Gamma)$, and the preytactic-sensitivity coefficient, $\chi(V, \Gamma)$. These make the constitutive equation for predator flux, equation (40), explicit, and this permits us to compute the spatiotemporal response of predators to heterogeneously distributed prey.

The only justification for our choice of equations (13) and (58) and for our ad hoc creation of the error function $\Omega(\Gamma)$ below is that they lead to good fits to our field data for the particular insect species we studied. Neither equation (13) nor equation (58) necessarily holds for other predator-prey systems. But alternative digestion and turning-behavior equations could be devised for other species, and their parameters could be estimated by a combination of experiments and best-fit routines similar to those we employ here.

TABLE 1

LADYBUG PREDATION AS A FUNCTION OF SATIATION AND APHID DENSITY

No. of Trials Averaged	Aphids per Meter, V	Starvation Time, τ (days)	Aphids Killed per Day (SD)	Model's Prediction of No. Killed	Error (%)
10	40	5.0	6.4 (11.0)	5.6	−12.6
5	60	0.25	0.0 (0.0)	8.2	200
12	115	0.5	4.0 (7.2)	14.7	114.3
8	130	1.0	28.0 (20.5)	16.3	−52.7
12	460	0.5	41.3 (33.0)	41.3	0.0
12	465	1.0	41.3 (23.0)	41.8	1.0
10	650	5.0	51.2 (45.8)	50.5	−1.4
14	2600	1.0	82.3 (53.6)	82.7	0.5
10	3350	5.0	99.2 (60.3)	87.0	−13.1
12	3350	2.0	89.3 (49.0)	87.0	−2.7
4	4350	1.0	92.0 (40.0)	90.5	−1.7
5	4530	1.0	92.8 (41.4)	91.0	−2.0
6	5600	5.0	90.7 (48.2)	93.5	3.1
10	5650	0.5	60.8 (32.6)	93.0	41.9
7	8630	0.25	50.3 (44.6)	95.9	62.4
10	44200	0.0	11.2 (17.0)	97.0	158.6
4	44200	0.25	68.0 (59.0)	102.1	40.1
10	48400	2.0	92.8 (48.2)	103.8	11.1
6	48400	5.0	104.0 (41.4)	103.8	−0.2
6	65600	1.0	104.0 (46.1)	104.0	0.0

NOTE.—Data are from the starvation/satiation experiments; each observation, lasting 30 min, was converted to a per-day rate.

Let $\aleph_1 = \{\psi_{\text{data}}(\tau_k, V_k) \mid k = 1, \ldots, N\}$ denote the set of N data points from the starvation/satiation experiments. Thus, the kth datum in $\aleph_1$, $\psi_{\text{data}}(\tau_k, V_k)$, represents the number of aphids eaten in 30 min by a ladybug starved for a time τ_k following satiation, when foraging in an aphid density of V_k. The first five columns of table 1 exhibit the ($N = 20$)–point data set $\aleph_1$ recorded in the present study.

With S elevated to the maximum possible value that equation (18) allows,

$$S = S_{\max} \equiv 1/(1 + \lambda/\gamma\nu) , \tag{60}$$

if satiated ladybugs starve while $V = 0$, they will end up with $S = S_{\max}e^{-\lambda\tau}$ after a time τ, according to equation (13). By the kill rate in equation (15), each ladybug should eat the following number of aphids during the $T = 30$-min interval over which we observed feeding:

$$\psi_{\text{model}}(\tau, V, T, \Gamma) = \int_0^T \left(\frac{\alpha\gamma V}{1 + V/\nu}\right)\left[\frac{1 - S(t)}{1 - \eta S(t)}\right] dt . \tag{61}$$

During this time, we assume that the aphid density, V, remains constant. During this feeding interval $0 < t < T$, the solution to equation (13), with initial condition $S(0) = S_{\max}e^{-\lambda\tau}$, is

$$S(t) = \theta/(\lambda + \theta) + [S_{\max}e^{-\lambda\tau} - \theta/(\lambda + \theta)]\, e^{-(\lambda+\theta)t} , \tag{62}$$

TABLE 2

DIRECTION REVERSALS OF INDIVIDUAL LADYBUGS AS A FUNCTION OF APHID DENSITY

No. of Trials Averaged	Aphids per Meter, V	No. of Reversals per Day (SD)	Model's Prediction of No. of Reversals	Error (%)	Model's Prediction of S
10	5	4.8 (6.7)	4.7	−40.2	.04
10	15	4.8 (15.1)	4.8	0.0	.10
10	25	7.2 (16.1)	5.5	−27.1	.16
14	25	5.1 (13.9)	5.5	6.3	.16
10	80	7.2 (11.5)	7.5	4.2	.36
14	100	8.6 (15.1)	8.9	3.3	.41
10	165	12.0 (17.0)	14.7	19.9	.52
8	420	45.0 (40.1)	34.7	−43.5	.68
15	500	25.6 (27.8)	38.9	41.2	.70
10	1140	69.6 (34.8)	56.3	−21.1	.78
21	5000	68.6 (35.0)	72.0	4.9	.832
32	25000	76.5 (39.6)	76.5	.02	.846
10	32710	84.0 (34.3)	76.9	−8.9	.847

NOTE.—Data are from the foraging-rule experiments; each observation, lasting 20 min, was converted to a per-day rate.

where

$$\theta \equiv \gamma V/(1 + V/\nu) . \tag{63}$$

Substituting this expression for $S(t)$ into equation (61), we can solve for the following explicit prediction of the number of aphids eaten by a ladybug in a time T if it had starved for a time τ after satiation before feeding:

$$\psi_{\text{model}}(\tau, V, T, \Gamma) = \frac{\alpha\theta}{\lambda + (1 - \eta)\theta} \times \left[\lambda T + \frac{1 - \eta}{\eta} \log\left(\frac{1 - \eta S_{\max} e^{-\lambda\tau}}{1 - \eta\{[\theta/(\lambda + \theta)](1 - e^{-(\lambda+\theta)T}) + S_{\max} e^{[-(\lambda+\theta)T - \lambda\tau]}\}}\right)\right] . \tag{64}$$

We wish to adjust the parameters in Γ such that $\psi_{\text{model}}(\tau, V, T, \Gamma) \approx \psi_{\text{data}}(\tau_k, V_k)$, for each $k = 1, \ldots, N$.

Let $\aleph_2 = \{R_{\text{data}}(V_j) \mid j = 1, \ldots, M\}$ denote the set of M data points from the foraging-rule experiments. Thus, the jth datum in $\aleph_2$, $R_{\text{data}}(V_j)$, represents the number of reversals per day by ladybugs experiencing a constant aphid density of V_j. The first three columns of table 2 exhibit the ($M = 13$)–point data set $\aleph_2$ of the present study. These data points are shown graphically in figure 1 above and in figure 3.

To wed the $\aleph_1$ and $\aleph_2$ measurements in tables 1–3 to our model, we went through a sequence of parameter-estimation exercises. First, we found the values of η, γ, λ, ν, and α that gave a best fit of the starvation/satiation data set, $\aleph_1$. Given these preliminary estimates, we used equation (18) to compute $S_0(V)$. We then plotted

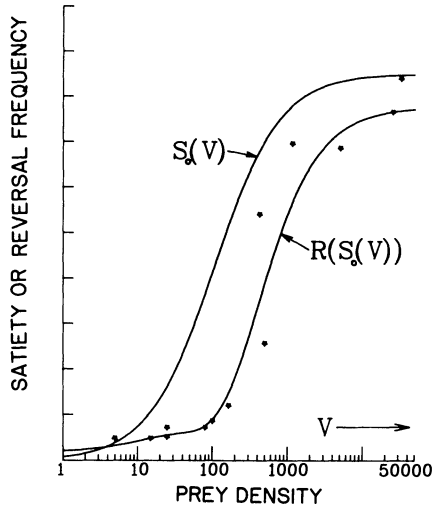

FIG. 3.—Predictions of the model using the best-fit parameter values. The upper curve shows the equilibrium satiety, $S_0(V)$, predicted by equation (18). The lower curve depicts the reversal frequency, $R[S_0(V)]$, predicted by the model equations (18) and (58). *Stars*, Experimental reversal data (see table 2). The horizontal axis measures the log of the aphid concentration density. The vertical axis has a dual linear scale, with S_0 ranging from 0 to 1.0 and R ranging from 0 to 100.

TABLE 3

HANDLING TIME AND CONSUMPTION RATES AS A FUNCTION OF APHID DENSITY

No. of Trials Averaged	Aphids per Meter, V	Average Handling Time per Aphid (s) (SD)	Average No. of Aphids Eaten per Day (SD)	Model's Prediction of No. Eaten	Error (%)
14	25	148.7 (67.0)	6.9 (14.6)	3.6	−62.5
14	100	93.1 (44.0)	24.0 (21.1)	12.9	−59.8
15	500	58.5 (41.0)	36.8 (41.5)	42.4	14.2
21	5000	23.6 (12.0)	102.9 (58.3)	87.0	−16.7
32	25000	24.7 (12.2)	96.0 (57.1)	96.0	0.0

NOTE.—Ladybugs foraged 4 h in known aphid densities before observation. Each observation, lasting 20 min, was converted to a per-day rate.

the reversal data in the set $\aleph_2$ versus S_0 to ascertain (by intuitive inspection) a reasonable functional form for the function $R(S)$. This revealed that a piecewise linear function would suffice, but, to avoid the undesirable discontinuity in dR/dS, we used the (smooth) polynomial function for $R(S)$, given in equation (58): $R(S) = \beta_0 + \beta_1 S + \beta_2 S^2 + \beta_3 S^3$.

We could proceed to find the values of β_0, β_1, β_2, β_3 that give a best fit of the reversal data set $\aleph_2$, while holding η, γ, λ, ν, and α fixed. But that would introduce a conceptual error because the function $R(S)$ in equation (58) depends on the

parameters η, γ, λ, and ν. The best values of these parameters for fitting the data in the set $\aleph_1$ may not be the best for fitting the set $\aleph_2$. Thus, we want to find the first nine parameters in $\Gamma = (\eta, \gamma, \lambda, \nu, \alpha, \beta_0, \beta_1, \beta_2, \beta_3, u)$ that simultaneously yield a best fit of the two distinct data sets $\aleph_1$ and $\aleph_2$. We accomplish this objective by minimizing the following error function, $\Omega(\Gamma)$, with respect to $\Gamma = (\eta, \gamma, \lambda, \nu, \alpha, \beta_0, \beta_1, \beta_2, \beta_3, u)$:

$$\Omega(\Gamma) = \frac{\omega}{N} \sum_{k=1}^{N} \left| \frac{\psi_{\text{data}}(\tau_k, V_k) - \psi_{\text{model}}(\tau_k, V_k, T, \Gamma)}{1 + \psi_{\text{model}}(\tau_k, V_k, T, \Gamma)} \right| + \frac{1 - \omega}{M} \sum_{j=1}^{M} \left| \frac{R_{\text{data}}(V_j) - R[S_0(V_j, \Gamma)]}{1 + R[S_0(V_j, \Gamma)]} \right| . \quad (65)$$

In equation (65), $R(S_0[V_j, \Gamma])$ denotes R as determined through equations (18) and (58), and ω is a weight factor between 0 and 1; the larger ω is, the less the reversal data count in determining the parameter vector Γ. We used $\omega = \frac{1}{2}$ to weight the two data sets $\aleph_1$ and $\aleph_2$ equally. The denominators in equation (65) normalize data that vary greatly in magnitude. Note that the predator-speed parameter, u, in Γ does not influence the function Ω. We used the capability of the ellipsoid algorithm to enforce nonlinear constraints among the parameters (see Ecker and Kupferschmid 1985) to find a minimum of $\Omega(\Gamma)$ satisfying these conditions: $\gamma > 0$; $0 \leq \eta < 1$; $\alpha > 0$; $\lambda > 0$; $\nu > 0$; $0 < \alpha < 8$; $dR/dS = \beta_1 + 2\beta_2 S + 3\beta_3 S^2 > 6$ for all $0 \leq S \leq 1$; and $S_{\max} > 0.85$.

With these constraints, the best minimizing values of the parameters we could find were $\eta = 0.9866$ (dimensionless), $\gamma = 0.018632$ m/day, $\nu = 711.2$/m, $\lambda = 2.3384$/day, $\beta_0 = 1.7115$, $\beta_1 = 45.3098$/day, $\beta_2 = -180.172$/day, $\beta_3 = 272.991$/day, and $\alpha = 8.00$/day. Throughout, we use units of days and meters. Tables 1–3 list details of the fit we achieved. Figure 1 depicts graphically our fit of the direction-reversal data, $\aleph_2$. Each of the last three constraints listed above was "active"; that is, the best fit we obtained could have been slightly improved if we relaxed any of those constraints. The others were inactive; relaxing them would make no difference in the final fit obtained, although they significantly "guided" the parameter-optimization search in its early steps. Without the constraint that $dR/dS > 6$, equation (67) below did not yield consistent determinations of the predator-speed parameter, u, from ladybug point-release experiments at different aphid densities.

Our point-release experiments for ladybugs yielded mean-squared dispersal distances in one day of $l^2 = 10\ \text{m}^2$ when the uniform aphid density was 5 aphids/m; and $l^2 = 6\ \text{m}^2$ when the uniform aphid density was 50 aphids/m. The mean-squared dispersal distance (l^2) and the dispersal coefficient (D) are related by the formula

$$2Dt = l^2 , \quad (66)$$

where t is the time during which particles (in this case, ladybugs) disperse. With $\partial V/\partial x = 0$, equations (41) and (66) yield

$$u = \{l^2 R[S_0(V)]/t\}^{1/2} . \quad (67)$$

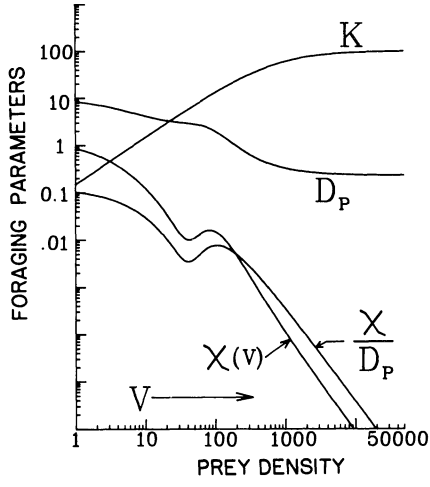

FIG. 4.—The single curve that climbs to the right shows the per-predator kill rate, $K[S_0(V), V]$, predicted by the model from equation (20). As for the three curves that decrease to the right, the upper curve shows the random-motility coefficient for ladybugs, $D_P(V)$, predicted by equation (41); the middle curve shows the preytactic-sensitivity coefficient, $\chi(V)$, predicted by equation (42); and the initially lowest curve shows the ratio $\chi(V)/D_P(V)$, appearing in equation (50). The vertical logarithmic scale is common to all four curves. Note, however, that all four quantities plotted are dimensional and have different units. $D_P(V)$ has units of m^2/day; $\chi(V)$ has units of m^3/day; $\chi(V)/D_P(V)$ is expressed in meters; and $K[S_0(V), V]$ has units of day^{-1}.

With the fit described above for R and $S_0(V)$, from which $R[S(V)] = 3.19$ and 6.19 when $V = 5$ and 50, respectively, equation (67) yields values for u of 5.65 m/day and 6.09 m/day, respectively. We use the average

$$u = 5.87 \text{ m/day} . \tag{68}$$

With all the parameters in Γ determined, we can use conditions (16)–(19) to compute the random-motility function, $D_P(V)$, from equation (41) and the preytactic-sensitivity function, $\chi(V)$, from equation (42). The results are shown graphically in figure 4.

RECIPES FOR PREDATOR AND PREY SOURCE-SINK TERMS COMPLETE THE POPULATION MODEL

In order to use the taxis model to predict macroscale predator-prey dynamics, we need to include aphid reproduction, aphid movement, ladybug immigration, and ladybug disappearance. The rate at which aphids are eaten has already been described by equation (57), whose parameters were estimated as part of the procedure for determining Γ. Aphid movement can be quantified by releasing large numbers of individuals at a particular point in a goldenrod row and observing the spread of the population. Before performing this experiment, we removed all other aphids from the goldenrod so that only our point-released aphids could

contribute to the estimate of dispersal rate. These experiments yielded an aphid-diffusion coefficient that varied a hundredfold, depending on weather, the age structure of the aphid population (early instars are sedentary, whereas adults are much more mobile), and quality of vegetation (from 0.01 m^2/day to 1 m^2/day). Because in our experiments most aphids were early instars, for the example that follows we have used an aphid diffusion coefficient of

$$D_V = 0.02 \text{ m}^2/\text{day} . \tag{69}$$

From sampling and manipulating aphid populations over the last 4 yr, we have some idea of the maximum densities attainable per goldenrod stem or per meter of goldenrod row. We use a maximum aphid density of $V_{\max} = 50{,}000$/m. To represent resource-limited growth, we describe net aphid production by

$$dV/dt = \sigma_{Vn}(V, P) = bV(V_{\max} - V) , \tag{70}$$

where b is the aphid growth parameter.

Equation (70) can be solved exactly for $V(t)$ if V_0 is known. That exact solution can be converted to the form

$$b = \ln \{V(t)(V_{\max} - V_0)/V_0[V_{\max} - V(t)]\}/V_{\max}t . \tag{71}$$

We used equation (71) to determine b by transplanting groups of aphids onto single, isolated goldenrod stems and keeping the stems clear of ladybugs for 11 days. We censused the aphid populations on each of 33 such stems shortly after the aphid transplantation (to measure V_0), 5 days later (to measure $V(t)$, with $t = 5$ days), and again 11 days later (to measure $V(t)$, with $t = 11$ days). The initially transplanted aphid populations, converted to equivalent units of aphids per meter in rows of contiguous stems, ranged from 120/m to 3440/m. The aphid densities measured after 5 days ranged from 160/m to 8260/m. The aphid densities after 11 days ranged from 1820/m to 44,560/m. The average of values for b calculated from equation (71) using the 5-day growth data was

$$b = 3.76 \times 10^{-6} \text{ m/day} , \tag{72}$$

with a standard deviation of 2.13×10^{-6}.

Ladybug immigration and disappearance is the final process that we need to consider. During the time periods we are considering, ladybug birth is negligible and thus can be ignored. To predict dynamics over the entire summer, birth and the predation behavior of each larval instar would, of course, need to be included as an input. The total number of ladybugs in a row of goldenrod is governed by the balance between immigration and disappearance, with the distribution of those ladybugs shaped by random movement and preytaxis. By removing all ladybugs from goldenrod rows and counting each arrival, we estimated that immigration ranged from 0.2 to 2.0 individuals per meter per day. This estimate varies with weather and date; for the cases of low aphid density and high aphid density described in the next subsection, we used, respectively,

$$\sigma_{Pa} = 0.5 \text{ per meter per day} \quad \text{and} \quad 0.2 \text{ per meter per day} \tag{73}$$

for exploratory numerical simulations. The immigration rate falls off sharply as the growing season progresses, and these different rates correspond to the differ-

ent weeks during which we performed the population experiments that we compare with our model in the next section. Since these ladybugs cannot detect aphids from distances greater than 1 cm (see Nakamuta 1985), immigration is not influenced by aphid density. But emigration (disappearance) does vary markedly with aphid density. If aphids are so scarce that ladybugs search for long periods without encountering one, then ladybugs are likely to take off on long emigration flights (i.e., leave the field; pers. obs.). Ladybugs, however, typically remain in a local patch of goldenrod where aphids are abundant. To describe this threshold emigration process, we take dP/dt because of disappearance or emigration to be

$$\min\{0, A_1(V - A_2)P\} . \tag{74}$$

The parameters in equation (65) were estimated by marking ladybugs and releasing them in goldenrod rows containing different densities of aphids, V. The fractions of ladybugs remaining after one day or half a day (both time intervals were used in these experiments) were then used to estimate A_1 and A_2 in equation (74). Before fitting equation (74) to the data, we corrected for the fact that approximately 17% of all released ladybugs leave as a result of the disturbance they suffer during marking and releasing. The parameters $A_1 = 0.0095$ m/day and $A_2 = 107.0$/m produced a maximum error of 28% and an average error of 7% with respect to predicted versus observed disappearance rates.

PREDICTIONS OF THE FULL MODEL RESEMBLE ACTUAL SPATIOTEMPORAL DYNAMICS MEASURED IN THE FIELD

We are now in a position to solve equations (55) and (56) since every parameter in them has been estimated. We have done this for two different sets of initial aphid and ladybug densities, which correspond to initial densities that we contrived experimentally along 10-m strips of goldenrod.

We controlled the initial density of aphids within each meter-long section by adding individuals or removing individuals as required. Our two sets of initial conditions involved low aphid densities in June 1985 (fig. 5) and high aphid densities in July 1985 (fig. 6). We released ladybugs at a uniform density of 1/m for the June experiment and 2/m for the July experiment. We then followed the spatiotemporal dynamics of these ladybug-aphid interactions over 2 days, censusing ladybugs in each meter 1 day and 2 days after the initial release of ladybugs. We had the time and manpower to census aphids only on day 2 of the June experiments. Each of these experiments used three replicates. When we compare model predictions to observed data, the observed data represent the averages of the three replicates. To minimize confounding influences, predators other than *Coccinella septempunctata* adults were removed from our experimental strips before each experiment. The test of our model is how well it predicts the rearrangement of the swarm of ladybugs (initially of uniform density) into the aggregations we observed (1 or 2 days later) at our experimentally created clumps of higher aphid density. There is no circularity in this test because our model was based on 20–30-min observations of individual ladybug behavior on goldenrod strips containing uniform densities of aphids. Thus, our spatially heterogeneous 2-

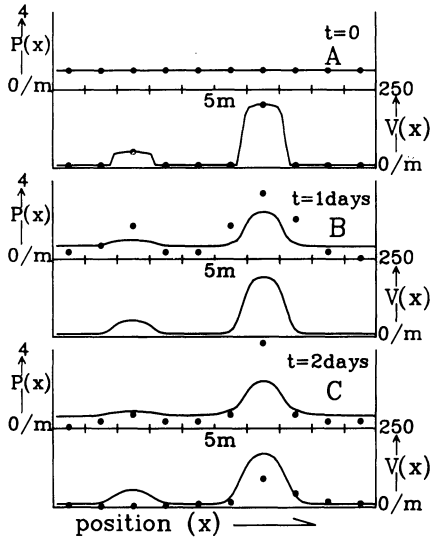

FIG. 5.—The June 1985 experiment. Spatial patterning of ladybugs in response to an experimentally contrived relatively low density aphid distribution in a 10-m-long, one-dimensional goldenrod strip. *A*, Conditions at the initial instant, $t = 0$; *B*, at $t = 1$ day; *C*, at $t = 2$ days. In each panel, the ladybug distribution, $P(x)$, is graphed above the aphid distribution, $V(x)$. *Dots*, Experimental observations (three independent measurements in three separate goldenrod strips, averaged). *A*, The line connecting the dots shows the initially uniform ladybug distribution (1/m). *B*, *C*, The curves show the predictions of our mathematical model after 1 and 2 days computed by solving the partial differential equations (55) and (56) with experimentally determined parameters, using the method of lines. No flux boundary conditions hold at both ends of the hedge.

day test is unlike the experiments we used to determine our model's parameter values.

Because ladybug density is so low in our experiments, the movement of one or two individuals can drastically alter the fit between model and data. It is peculiar even to think of 1–3 ladybugs per meter in terms of a continuum population model. But we interpret the predicted densities of ladybugs as a probability density distribution; if our model is appropriate, ladybugs, on the average, should be distributed in space in accordance with the model predictions.

The match between our experimental observations and model predictions is presented in figure 5 (low density) and figure 6 (high density). Testing the model rigorously would require an ensemble of many more than three experiments, whose average behavior we could compare to model predictions. The data in figures 5 and 6 do not represent such an ensemble. We present these figures mainly to indicate that the data are not ridiculously out of line with our theory and to illustrate how our model can be applied to predator-prey systems in the field. The point is that the model stems from concrete observations of individual behavior and yields unambiguous, testable predictions about predator distributions relative to patchily distributed prey.

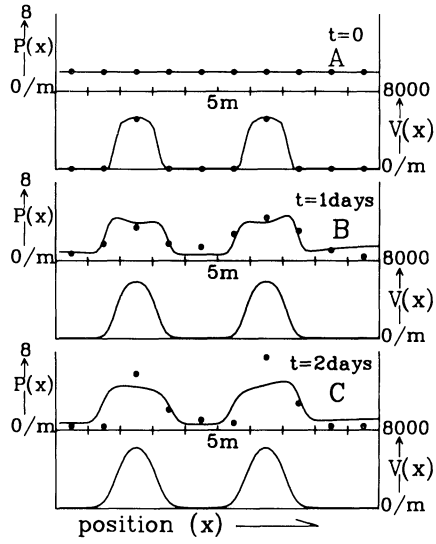

FIG. 6.—The July 1985 experiment. Spatial patterning of ladybugs in response to a relatively high density aphid distribution in a 10-m-long, one-dimensional goldenrod strip. This is the same type of plot as in figure 5, but the aphid densities are much higher (peaks of 5000 aphids per meter at $t = 0$). There are twice as many ladybugs in the strip initially as in figure 5.

Since solving nonlinear partial differential equations is an expensive process, below we explain a mathematical shortcut to show that our new preytaxis model of area-restricted search does predict aggregation of predators at peaks in prey density. We compute the steady-state spatial distribution that a swarm of ladybugs adopts in response to a time-invariant spatial distribution of aphids. That is, we establish experimentally a known aphid distribution along a goldenrod row, and we ignore equation (55). With $V(x)$ fixed, we consider the steady-state distribution, $P(x)$, to which the solution of equation (56) tends as t approaches infinity. From solving the full partial-differential-equation system, we know that the "t approaches infinity" solution is nearly attained in about one day.

There are two ways to compute steady-state solutions to equation (56) when $V(x)$ is fixed. We can assume no ladybug immigration and emigration and calculate $P(x, t)$ as t approaches infinity, using equation (49). Alternatively, we can permit arbitrary predator immigration and emigration and still solve equation (56) for $P(x)$. The latter solution is harder to obtain than the explicit solution of equation (49); Appendix B explains how this is done. As explained above, equation (49) cannot tell us how many ladybugs should be in the goldenrod row at equilibrium; the procedure in Appendix B does this, however, and that is the procedure we used to generate the graphs in figure 7, which show two examples in a domain 10 m long containing aphid clusters and a population of ladybugs. For the particular parameter values we used and the experimentally contrived low-density aphid population distribution, the explicit and simple equation (49), adjusted to have the

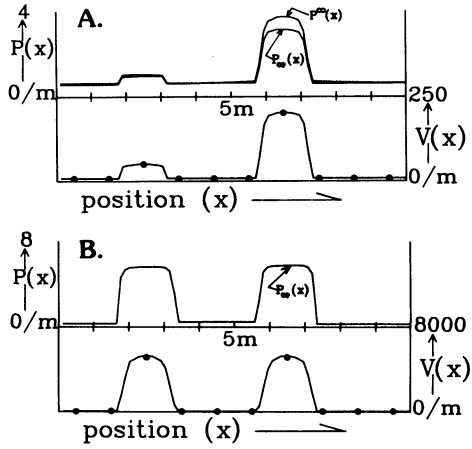

FIG. 7.—Steady-state solutions. The curve labeled $P_\infty(x)$ shows the steady-state ladybug distribution predicted by equation (49) as t approaches zero with the aphid distribution frozen in time and no ladybug emigration or immigration. The curve labeled $P^\infty(x)$ shows the steady-state ladybug distribution predicted as t approaches infinity with aphid distribution frozen in time but with both ladybug emigration and immigration. The procedure for computing this solution is given in Appendix B. *A*, The steady-state fit to the June experiment with a lower aphid density; *B*, the steady-state fit to the July experiment with a higher aphid density.

same net predator population, gave a steady-state solution similar to the one generated by the more-complicated boundary-value-problem solution technique given in Appendix B. These steady-state solutions approximate the solutions of the partial differential equations shown in figures 5 and 6. All these solutions demonstrate clearly that our area-restricted search leads to dramatic predator aggregation through preytaxis.

DISCUSSION

Clearly, our estimation of model parameters and testing of the model need further work. We have, however, demonstrated an approach that we think is extremely useful for studying spatially distributed predator-prey systems. Some notable limitations of the model deserve comment. Both our analyses of area-restricted search and the partial differential equations that are obtained from that behavior represent only one spatial dimension. Conceptually, there is no problem adapting our approach to two dimensions. We restricted ourselves to one dimension because it made both the experiments and the computations simpler. In practice, a two-dimensional formulation may become much more tedious. We are in the process of developing such a formulation and determining whether it is even needed to investigate the effectiveness of predators as control agents for prey or pest populations.

In our view, a more substantive problem is our neglect of the role of stochastic factors in predator-prey interactions. Our only remedy for this defect is to interpret our model's predictions cautiously, as though they applied only to the

averaged behavior of an ensemble of experiments. Direct stochastic approaches to predator-prey or to spatially distributed systems are just beginning to be explored and are still at too early a stage of development to be applied to specific field systems (for reviews of this subject, see Chesson 1978, 1985).

We intend to use our model primarily to compare the effectiveness with which different ladybug species contain incipient outbreaks of their prey. Of course, the results of such comparisons depend on the initial population of predators, on the shape and size of the prey species' outbreak, and on the background density of prey surrounding the outbreak. Different predators might be seen as being predisposed to take advantage of (aggregate at) prey eruptions of different sizes. If so, one might use models such as equations (55) and (56) to identify ideal suites of predators for biological control in different agricultural systems. The idea of relating individual behavior to the ability of predators to regulate their prey is not new. Over a decade ago, Hassell and May (1974) urged population ecologists to relate the overall dynamics of predator-prey systems to detailed observations of predator foraging behavior; they also developed a model that did exactly that, focusing, as we have, on area-restricted search. But whereas Hassell and May modeled predators moving between discrete patches of habitat, we have treated the interaction in a continuum. Nonetheless, following a totally different argument, Hassell and May (1974) also showed that area-restricted search behavior leads to aggregations of predators in regions of high prey density.

Often, when examining aggregation and predator-prey systems, theoreticians concern themselves with "stability" (see, e.g., Hassell and May 1985; Chesson and Murdoch 1986). We purposely avoid making any statements about the effects of aggregation on stability. One reason for this is that our model can be extrapolated reliably to characterize year-to-year dynamics only by including much more information than we have measured about ladybug and aphid birth and growth rates (including the dynamics of ladybug birth and metamorphosis). In addition, we are concerned primarily with questions that relate to transient dynamics, such as the short-term fate of a prey eruption in a single agricultural field.

Nevertheless, we feel that the kind of model presented here provides the proper theoretical frame within which to pose and answer questions about how aggregation affects stability. Solutions to our model's equations, integrated over the spatial domain, yield the total population of both predator and prey at each time; thus, they can predict gross population cycles or equilibria and can assess, numerically at least, the differences in those cycles caused by increased or diminished aggregation. Although we have not initiated such a study, we feel that we have established the appropriate combination of mathematical and field-study tools for the task.

Finally, we avoid general remarks about the effect of aggregation on stability because we think it is unlikely that there are simple general principles about the effect of aggregation on the stability of predator-prey systems; differences in the detailed behavior of the species involved could lead to opposite verdicts. For instance, numerical solutions to our model's equations indicate clearly that although a predator may aggregate at prey, this does not mean that the predator-arrival rate necessarily increases with increasing prey density. It is possible for

prey population growth to swamp predator aggregation, leading to a decline in predation rates over some regions of increasing prey density. However satisfying they may seem, simple theoretical predictions are unlikely to be valid for the panoply of behaviors subsumed under the rubric *predator aggregation*.

A conditional case-by-case theory, founded on field measurements of the parameters characterizing individual predator and prey movement and birth-death dynamics, capable of predicting spatial aggregation patterning and, ultimately, the effects on whole-population stability is now within reach. We hope that this paper helps to steer future empirical and mathematical research toward that type of mechanistic theory. In these efforts, attention to the dimension of the physical domain (one, two, or three) and spatial processes (turning-angle distribution as well as turning frequency) will be imperative, through both partial differential equations and direct observations of animal movement.

A failure of predation to contain an incipient prey outbreak can be interpreted as predation causing patchiness in prey distribution. Indeed, this may be an important theoretical consequence of the model presented in this paper. It is simple and instructive to connect our model in general abstract terms to a large body of literature on pattern formation driven by "short-range activation" coupled with "long-range inhibition." A common conceptual thread linking many apparently diverse examples of spatial patterning consists of an "activating" or "excitatory" factor (aphids in our model) that increases autocatalytically (more activator leads to an increase in activator production rate); an "inhibitory" factor (ladybugs in our model), whose local "production" is triggered by the activator, that acts to inhibit activator production; and some mechanism whereby the inhibitor spreads significantly faster than the activator does.

Whenever these features are coupled, almost independently of the details of the physical processes responsible for them, spatial patterns are likely to form spontaneously. The patterns arise since, once ignited, the autocatalytic production of activator, confined laterally by the relatively slow spread of activator, locally overwhelms the inhibitor's capacity to suppress it. This is because the inhibitor, whose production is triggered by the activator peak, rapidly "leaks away" laterally. Thus, each activator peak that erupts is quickly surrounded by a broad domain of elevated inhibitory factor. This inhibitor elevation suppresses neighboring activator peaks. Usually such pattern-formation models involve an initial steady state that is spatially homogeneous and unstable when infinitesimally perturbed. Random initial perturbations grow into stable spatial patterns. (For diverse examples of this kind of pattern formation in action, see Meinhardt 1982; Ermentrout et al. 1986.) This paper begins to provide another example because each of the three required ingredients is present in the aphid-ladybug interaction.

1. We showed above that the logistic aphid reproduction with the kind of ladybug predation we measured results in autocatalytic net aphid reproduction dynamics (at low aphid and ladybug densities). That is, when V and P are low,

$$\partial[\sigma_{Vn}(V, P) - \sigma_{VK}(V, P)]/\partial V > 0 .$$

2. Ladybug aggregation via preytaxis in regions of elevated aphid density can be interpreted as an activator (aphids) triggering inhibitor "production." Further-

more, according to equations (73) and (74), the elevated aphid density means elevation of the ratio of predator immigration to emigration.

3. In our model and in our experiments, the aphid dispersal rate is much slower than the ladybug dispersal or aggregation rate.

We feel that, in this way, area-restricted-search predation might *explain* the patchiness observed in prey distributions in an otherwise homogeneous vegetation domain. In our model, the mechanism for initiating the formation of a pattern is not linear instability of a spatially homogeneous initial state. Instead, our model explains how a prey outbreak, started by a small aphid settlement early in the growing season, can grow to a very dense aphid population, isolated in the middle of uninfected vegetation. By attracting ladybugs, an aphid peak suppresses aphid outbreaks in its immediate vicinity.

SUMMARY

We show that if individual predators restrict the area of their search following an encounter with prey, then this behavior translates into populations of predators flowing toward regions of high prey density. This result requires only that predators move at a constant speed but change their direction of movement more often when their stomachs are full and that increases in prey density increase the feeding rate and stomach fullness of predators. The partial differential equation that is derived by assuming such behavior includes terms representing both random motion and taxis on the part of the predator. The form and magnitude of these terms can be estimated by quantifying how prey density influences the frequency of directional changes in a foraging predator and by obtaining functional-response curves for predators that have been starved for different lengths of time. In general, the strength of a predator's taxis or aggregation response depends on its average velocity of search and on the sensitivity of its turning frequency to changes in prey density, both of which are easily measured. Thus, we show how short-term observations of individual predators can lead to a complete macroscopic description of predator-prey interactions in a spatially distributed environment.

We demonstrate the use of our model by applying it to the spatial dynamics of an interaction between goldenrod aphids (*Uroleucon nigrotuberculatum*) and adult ladybug beetles (*Coccinella septempunctata*). Although in this specific case the model is limited to predictions on the order of weeks, we show how it might be used to evaluate the effectiveness of different predators as biological control agents. Our particular mechanistic model indicates that the consequences of aggregation for prey control depend on the rates of taxis relative to the rates of prey population growth; only sometimes is predator aggregation sufficient to halt an incipient prey outbreak.

ACKNOWLEDGMENTS

P. Chesson offered detailed and significant criticism that triggered a major reorganization of the paper. Comments by R. May, S. Levin, L. Segel, and two

anonymous referees greatly improved the final version. We thank P. Bierzychudek, J. Kingsolver, N. Cappuccino, and J. Bergelson for comments on a preliminary version of this manuscript. S. Mack carried out very useful exploratory numerical solutions of the partial differential equations. K. Odell and H. Surowiec helped to purge careless language from the manuscript. S. Wawrzynski provided more detailed and careful editorial assistance than either author has experienced heretofore.

Both authors were supported by the National Science Foundation (NSF) grant BSR 8517183. Both authors gratefully acknowledge the financial support provided by the Science and Engineering Council of Great Britain, through grant GR/C/63595. We thank J. D. Murray and the Centre for Mathematical Biology at the University of Oxford for the hospitality they extended. Work by G.O. was also supported by a Guggenheim Fellowship and NSF grant MCS 83-01460.

APPENDIX A

We sequester here the mathematical details by which the three differential equations (3), (35), and (36), plus the algebraic equation (2), can be collapsed to the pair of algebraic equations (37) and (38). This is possible when certain near-equilibrium conditions hold. We suppose a mild gradient in $V(x)$ to be imposed and held constant in time. We suppose that a few predators wander on this V gradient. Finally, we suppose, initially at least, that the gradient $\partial P/\partial x$ remains close to zero (i.e., the predators are uniformly distributed). Although these special conditions cannot persist for long without outside intervention, they tell us what the reversal probabilities, $r^{\Rightarrow}$ and $r^{\Leftarrow}$, are for the typical right- or left-moving predator. There is an implicit assumption here that the predators do not sense directly the gradient of their own population distribution, but each individual behaves in a predator gradient as it would behave in a spatially uniform distribution of predators at the same local density.

$\partial P/\partial t = 0$ and $\partial P/\partial x \ll 1$ reduce equation (28) to

$$J_P = P\left(\frac{r^{\Leftarrow} - r^{\Rightarrow}}{r^{\Leftarrow} + r^{\Rightarrow}}\right) u \,, \tag{A1}$$

from which equations (26) and (27) reduce to

$$n^{\Rightarrow} = P\left(\frac{r^{\Leftarrow}}{r^{\Rightarrow} + r^{\Leftarrow}}\right) \quad \text{and} \quad n^{\Leftarrow} = P\left(\frac{r^{\Rightarrow}}{r^{\Rightarrow} + r^{\Leftarrow}}\right). \tag{A2}$$

These, substituted in turn into equations (35) and (36), yield

$$\partial S^{\Rightarrow}/\partial t + u\,\partial S^{\Rightarrow}/\partial x = -r^{\Rightarrow}(S^{\Rightarrow} - S^{\Leftarrow}) + f(S^{\Rightarrow}, V) \tag{A3}$$

and

$$\partial S^{\Leftarrow}/\partial t - u\,\partial S^{\Leftarrow}/\partial x = r^{\Leftarrow}(S^{\Rightarrow} - S^{\Leftarrow}) + f(S^{\Leftarrow}, V) \,. \tag{A4}$$

We now introduce two names: $g \equiv S^{\Rightarrow} - S^{\Leftarrow}$, for the satiety difference between right- and left-moving predators; and $\Sigma \equiv S^{\Rightarrow} + S^{\Leftarrow}$, for the satiety sum (which turns out to be twice its average). We add equations (A3) and (A4) to obtain

$$\partial\Sigma/\partial t + u\,\partial g/\partial x = (r^{\Leftarrow} - r^{\Rightarrow})g + f(S^{\Rightarrow}, V) + f(S^{\Leftarrow}, V) \,. \tag{A5}$$

Subtraction of equation (A4) from equation (A3) produces

$$\partial g/\partial t + u\,\partial\Sigma/\partial x = -(r^{\Leftarrow} + r^{\Rightarrow})g + f(S^{\Rightarrow}, V) - f(S^{\Leftarrow}, V) \,. \tag{A6}$$

For the special circumstances under consideration, wherein $V(x)$ is held fixed independent of time, we expect all quantities to approach an equilibrium value as t approaches

infinity, and therefore we expect $\partial\Sigma/\partial t = \partial g/\partial t = 0$ in equations (A5) and (A6). If $\partial V/\partial x$ is not too steep, $\partial S_0/\partial t$ is not too large, and the predator speed, u, is not too fast; then we expect, at each position x, to have both $S^{\Rightarrow}$ and $S^{\Leftarrow}$ close to $S_0(V)$. That is, we expect $|g|$ to be small. If so, we can expand quantities such as $r^{\Rightarrow} = R(S^{\Rightarrow})$, $r^{\Leftarrow} = R(S^{\Leftarrow})$, $f(S^{\Rightarrow}, V)$, $f(S^{\Leftarrow}, V)$, and so forth, in a Taylor series around the $S_0(V)$ equilibrium value, which we now do, keeping terms up to order g^2 and neglecting higher-order terms. We obtain

$$r^{\Leftarrow} - r^{\Rightarrow} \approx - dR\,[S_0(V)]g/dS\ , \tag{A7}$$

$$f(S^{\Rightarrow}, V) - f(S^{\Leftarrow}, V) \approx \frac{\partial f}{\partial S}\,[S_0(V), V]g\ , \tag{A8}$$

$$f(S^{\Rightarrow}, V) + f(S^{\Leftarrow}, V) \approx 2f[S_0(V), V] + \frac{1}{4}\,\frac{\partial^2 f}{\partial S^2}\,[S_0(V), V]g^2\ . \tag{A9}$$

But $f[S_0(V), V] = 0$ by the definition of S_0. Thus,

$$r^{\Rightarrow} + r^{\Leftarrow} \approx 2R[S_0(V)] + \frac{1}{4}\,\frac{d^2R}{dS^2}[S_0(V)]g_2\ , \tag{A10}$$

$$\frac{\partial\Sigma}{\partial x} = \frac{\partial}{\partial x}\,(S^{\Rightarrow} + S^{\Leftarrow}) \approx 2\,\frac{dS_0}{dV}\,(V)\,\frac{\partial V}{\partial x}\ . \tag{A11}$$

When equations (A8), (A10), and (A11) are substituted into equation (A6), we find that

$$g = 2u\,\frac{dS_0}{dV}(V)\frac{\partial V}{\partial x}\Big/\left\{\frac{\partial f}{\partial S}\,[S_0(V), V] - 2R[S_0(V)]\right\}\ . \tag{A12}$$

When equation (A12) is substituted into equation (A7), we get

$$r^{\Leftarrow} - r^{\Rightarrow} = 2u\,\frac{dR}{dS}\,[S_0(V)]\,\frac{dS_0}{dV}\,\frac{\partial V}{\partial x}\Big/\left\{2R[S_0(V)] - \frac{\partial f}{\partial S}\,[S_0(V), V]\right\}\ . \tag{A13}$$

If we now substitute equations (A13) and (A10), with the g^2 term neglected, into equation (29), we obtain equation (39), which is our main result. It remains only to check that equation (A5), the other conservation rule for $S^{\Rightarrow}$ and $S^{\Leftarrow}$, is consistent with equation (A12) to at least first order in g. It is, because when we substitute equations (A10) and (A11) into equation (A6), we obtain

$$\frac{\partial g}{\partial x} = \frac{1}{u}\left\{\frac{1}{4}\,\frac{\partial^2 f}{\partial S^2}\,[S_0(V), V] - \frac{dR}{dS}\,[S_0(V)]\right\}g^2\ . \tag{A14}$$

Strictly speaking, equation (A14) contradicts equation (A12) unless very special choices are made for the functions $R(S)$ and $f(S, V)$. However, the disagreement between equations (A14) and (A12) is a negligible quantity of order g^2, and so it does not damage our approximation scheme.

APPENDIX B

In this appendix, we explain how to solve for the eventual (t approaches ∞) steady-state distribution of predators in the special case when a fixed (time-invariant) distribution $V(x)$ of prey is maintained (by experimental contrivance or because there are too few predators to affect the prey population). Equation (49) does this in the trivial case when the net predator source-sink term, σ_P, equals zero. Here, we treat the much more complex steady-state problem when σ_P is an arbitrary nonvanishing function. Though more complicated than equation (49), this problem involving an ordinary differential equation (ODE) is much simpler than the problem involving a full partial differential equation (PDE).

Our preliminary experience with solving the system of full partial differential equations (55) and (56) shows that, following initial transients, at each time t, the time-dependent predator distribution, $P(x, t)$, is close to the steady-state solution computed below, which

would correspond to the prey distribution $V(x, t)$ at that time t if $V(x, t)$ were held "frozen" with respect to t. Thus, the solution to the ordinary differential equation below can give a good estimate of what snapshots of the PDE system's solutions should look like at a sequence of instants.

We suppose $V(x)$ is prescribed on a domain $0 < x < L$. We seek the steady-state ($\partial P/\partial t = 0$) solution as t approaches infinity to equation (56). Thus, we want to solve the ODE,

$$dJ_P/dx = d[-D_P(V)dP/dx + P\chi(V)dV/dx]/dx = \sigma_P(V, P), \tag{B1}$$

for $0 \leq x \leq L$. Suppose no flux of predators can penetrate the ends of the domain (i.e., $J_P = 0$ at $x = 0$ and at $x = L$).

We convert the second ODE (B1) into a system of two first-order ODE's by defining

$$z_1(x) = P(x) \tag{B2}$$

and

$$z_2(x) = -D_P(V)dP/dx + P\chi(V)dV/dx. \tag{B3}$$

The term $z_2(x)$ is just the flux density of predators. Then, we solve the following ODE system of two autonomous first-order equations:

$$dz_1/dx = z_1\chi[V(x)]dV/dx - z_2(x)/D_P[V(x)] \equiv F_1(z_1, z_2), \tag{B4}$$

$$dz_2/dx = \sigma_P(V, z_1) \equiv F_2(z_1, z_2), \tag{B5}$$

which is equivalent to equation (B1), subject to the boundary conditions

$$z_2(0) = z_2(L) = 0. \tag{B6}$$

This we solve using the "shooting method." We introduce the name ζ for the unknown initial value of $P(0)$; and for any positive ζ, we solve the initial-value problem consisting of equations (B4) and (B5) with the initial conditions

$$z_1(0) = \zeta \quad \text{and} \quad z_2(0) = 0. \tag{B7}$$

This gives a numerically computed solution that depends on ζ, which we denote by

$$\{z_1(x, \zeta), z_2(x, \zeta)\}.$$

We then use any standard root-finding method (such as Newton's method, Muller's method, or even the bisection method) to adjust ζ to find a zero of the function

$$H(\zeta) \equiv z_2(L, \zeta). \tag{B8}$$

For the unique value of ζ satisfying equation (B8), the solution of the initial-value problem (with $z_1(0) = \zeta$) is also the solution of the no-flux, boundary-value problem of equations (B4), (B5), and (B6).

Such a solution is shown in figure 6*a*. It is similar to the explicit solution given in equation (49). Thus, at least for the data fit we measured for ladybugs and aphids, the easy, explicit calculation of equation (49) gives a good estimate of how ladybugs are expected to aggregate in the vicinity of local aphid concentrations as a consequence of area-restricted search, whether or not emigration and immigration occur.

LITERATURE CITED

Alt, W. 1980. Biased random walk models for chemotaxis and related diffusion approximations. J. Math. Biol. 9:147–177.

Banks, C. 1957. The behavior of individual coccinellid larvae on plants. Br. J. Anim. Behav. 5:12–24.

Banks, H. T., P. Kareiva, and P. Lamm. 1985. Modeling insect dispersal and estimating parameters when mark-release techniques may cause initial disturbance. J. Math. Biol. 22:259–277.

Broadbert, S., and D. Kendall. 1953. The random walk of *Trichostrongylus retortaeformis*. Biometrics 9:460–466.

Carter, M., and A. F. G. Dixon. 1982. Habitat quality and the foraging behavior of coccinellid larvae. J. Anim. Ecol. 51:865–878.
———. 1984. Foraging behavior of coccinellid larvae: duration of intensive search. Entomol. Exp. Appl. 36:133–136.
Chandler, A. 1969. Locomotory behavior of first instar aphidophagous Syrphidae (Diptera) after contact with aphids. Anim. Behav. 17:673–678.
Chesson, P. 1978. Predator-prey theory and variability. Annu. Rev. Ecol. Syst. 9:323–347.
———. 1985. Environmental variation and the coexistence of species. Pages 240–256 *in* J. Diamond and T. Case, eds. Community ecology. Harper & Row, New York.
Chesson, P., and W. Murdoch. 1986. Aggregation of risk: relationships among host-parasitoid models. Am. Nat. 127:696–715.
Cook, R., and B. Cockrell. 1978. Predator ingestion rate and its bearing on feeding time and the theory of optimal diets. J. Anim. Ecol. 47:529–547.
Curio, E. 1976. The ethology of predation. Springer-Verlag, New York.
Ecker, J. G., and M. Kupferschmid. 1985. A computational comparison of the ellipsoid algorithm with several non-linear programming algorithms. SIAM (Soc. Ind. Appl. Math.) J. Control Optimization 23:657–674.
Ermentrout, B., J. Campbell, and G. Oster. 1986. A model for shell patterns based on neural activity. Veliger 28:369–388.
Fisher, R. 1937. The wave of advance of advantageous genes. Ann. Eugen. 7:355–369.
Fleschner, C. 1950. Studies on the searching capacity of the larvae of three predators of the citrus red mite. Hilgardia 20:233–265.
Gutierrez, A., C. Summers, and J. Baumgaertner. 1980. The phenology and distribution of aphids in California alfalfa as modified by ladybird beetle predation. Can. Entomol. 112:489–495.
Hassell, M. 1978. The dynamics of arthropod predator-prey systems. Princeton University Press, Princeton, N.J.
———. 1985. Insect natural enemies as regulating factors. J. Anim. Ecol. 54:323–334.
Hassell, M., and R. May. 1974. Aggregation in predators and insect parasites and its effect on stability. J. Anim. Ecol. 43:567–594.
———. 1985. From individual behavior to population dynamics. Br. Ecol. Symp. 18:3–32.
Heads, P., and J. Lawton. 1983. Studies on the natural enemy complex of the holly leaf miner: the effects of scale on the detection of aggregative responses and the implications for biological control. Oikos 40:267–276.
Holling, C. S. 1965. The functional response of predators to prey and its role in mimicry and population regulation. Mem. Entomol. Soc. Can. 45:1–60.
Kareiva, P. 1982. Experimental and mathematical analyses of herbivore movement: quantifying the influence of plant spacing and quality on foraging discrimination. Ecol. Monogr. 52:261–282.
———. 1984. Predator-prey dynamics in spatially-structured populations: manipulating dispersal in a coccinellid-aphid interaction. Lect. Notes Biomath. 54:368–389.
———. 1985. Patchiness, dispersal, and species interactions: consequences for communities of herbivorous insects. Pages 192–206 *in* J. Diamond and T. Case, eds. Community ecology. Harper & Row, New York.
Keller, E. F., and L. A. Segel. 1970. Initiation of slime mold aggregation viewed as an instability. J. Theor. Biol. 26:399–415.
———. 1971. Traveling bands of chemotactic bacteria: a theoretical analysis. J. Theor. Biol. 30: 235–248.
Lapidus, I. 1980. "Pseudochemotaxis" by micro-organisms in an attractant gradient. J. Theor. Biol. 86:91–103.
Lauffenberger, D., and R. Aris. 1979. Measurement of leukocyte motility and chemotaxis parameters using a quantitative analysis of under-agarose migration. Math. Biosci. 44:121–138.
Levin, S. 1981. The role of theoretical ecology in the description and understanding of populations in heterogeneous environments. Am. Zool. 21:865–875.
Meinhardt, H. 1982. Models of biological pattern formation. Academic Press, New York.
Murdie, G., and M. Hassell. 1973. Food distribution, searching success, and predator-prey models.

Pages 87–101 *in* R. Hiorsn, ed. The mathematical theory of the dynamics of biological populations. Academic Press, London.

Murdoch, W. 1975. Diversity, complexity, stability and pest control. J. Appl. Ecol. 12:795–807.

Murdoch, W., J. Chesson, and P. Chesson. 1985. Biological control in theory and practice. Am. Nat. 125:344–366.

Nakamuta, K. 1985. Behavioral mechanism of switchover in search behavior of the ladybeetle, *Coccinella septempunctata*. J. Insect Physiol. 31:849–856.

Namba, T. 1980. Density-dependent dispersal and spatial distribution of a population. J. Theor. Biol. 86:351–363.

Obrycki, J., J. Nechols, and M. Tauber. 1982. Establishment of a European ladybeetle in New York State. N.Y. Food Life Sci. Bull. 94:1–3.

Okubo, A. 1980. Diffusion and ecological problems: mathematical problems. Springer-Verlag, New York.

Segel, L. A. 1977. A theoretical study of receptor mechanisms in bacterial chemotaxis. SIAM (Soc. Ind. Appl. Math.) J. Appl. Math. 32:653–665.

———. 1984. Taxes in cellular ecology. Lect. Notes Biomath. 54:407–424.

Sih, A. 1980. Optimal foraging: partial consumption of prey. Am. Nat. 116:281–290.

Skellam, J. 1951. Random dispersal in theoretical populations. Biometrika 38:196–218.

Smith, J. 1971. Studies of the searching behavior and prey recognition of certain vertebrate predators. Ph.D. diss. University of Oxford, Oxford.